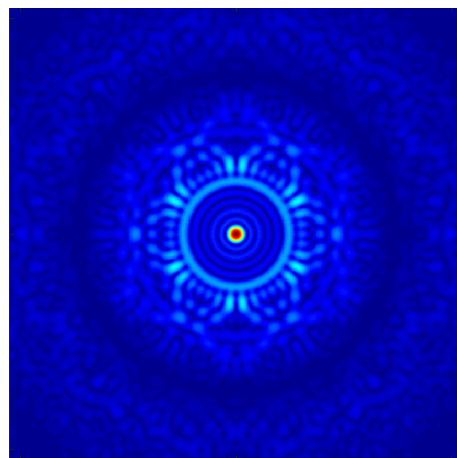




Fundamental course: Fourier Optics

Lecture notes

Revision date: August 27, 2018



Simulation of the Point-Spread Function of a 39 pupils interferometer, with sub-apertures disposed on 3 concentric rings.

Contents

0 Reminders about Fourier analysis	4
0.1 Some useful functions	4
0.1.1 The rectangle function	4
0.1.2 Dirac delta distribution	5
0.1.3 Dirac comb	6
0.2 Convolution	7
0.2.1 Definition	7
0.2.2 Properties	7
0.3 Fourier transform	9
0.3.1 Definition	9
0.3.2 Properties	10
0.3.3 Table of Fourier transforms	11
1 Reminders about diffraction	12
1.1 Some particular kinds of waves	12
1.1.1 Monochromatic waves	12
1.1.2 Plane waves	12
1.1.3 Spherical waves	13
1.2 Huyghens-Fresnel principle	16
1.2.1 Introduction	16
1.2.2 Paraxial approximation and Fresnel diffraction	16
1.2.3 Far field: Fraunhofer diffraction	17
1.2.4 Example of Fraunhofer diffraction patterns	18
2 Fourier properties of converging lenses	22
2.1 Phase screens	22
2.1.1 Transmission coefficient of a thin phase screen	22
2.1.2 Example: prism	23
2.1.3 Converging lens	23
2.2 Converging lenses and Fourier transform	24
2.2.1 Object in the same plane as the lens	25
2.2.2 Object at the front focal plane	25
3 Coherent optical filtering	27
3.1 Principle	27
3.2 Abbe-Porter experiments	27
3.3 Object-image relation	29
3.4 Low-pass and high-pass filters	30
3.4.1 Low-pass filters	30
3.4.2 High-pass filters	32
3.5 Strioscopy and phase contrast	32
3.5.1 Strioscopy	33
3.5.2 Phase contrast	34

4	Image formation	35
4.1	Object-image convolution relation	35
4.1.1	Image created by a point-source	35
4.1.2	Object-image relation	37
4.2	Optical transfer function (OTF)	38
4.3	Case of a circular pupil	40
4.3.1	PSF and resolving power	40
4.3.2	Optical transfer function	41

Chapter 0

Reminders about Fourier analysis

Also read:

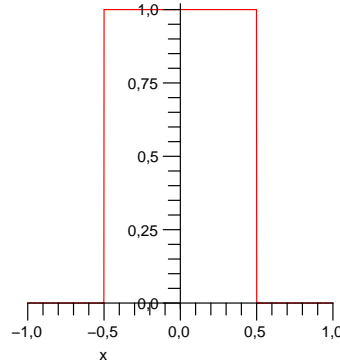
- Bracewell, R. “The Fourier Transform and its applications”
- Goodman, J.W. “Introduction to Fourier Optics”, chap 2
- Roddier, F., “Distributions et transformation de Fourier” (in french)

0.1 Some useful functions

0.1.1 The rectangle function

The rectangle function is useful to describe objects like slits or diaphragms whose transmission is 0 or 1. It is defined as

$$\begin{aligned}\Pi(x) &= 1 \text{ if } |x| < \frac{1}{2} \\ \Pi(x) &= 0 \text{ otherwise}\end{aligned}\quad (1)$$



Some other definitions may be found in the literature (in particular for the value at $x = \pm\frac{1}{2}$). A rectangular function of width a centered at $x = b$ will express as $\Pi\left(\frac{x-b}{a}\right)$.

2D rectangle function

We consider functions of 2 variables x and y . The quantity

$$f(x, y) = \Pi(x) = \Pi(x) \mathbf{1}(y)$$

describes a strip of width 1 parallel to the y axis : it is invariant by translation along y (see Fig. 1). The notation $\mathbf{1}(y)$ stands for a function which value is 1 whatever y .

A two dimensional rectangle function of width a in the x direction and b in the y direction expresses as

$$f(x, y) = \Pi\left(\frac{x}{a}\right) \Pi\left(\frac{y}{b}\right) \quad (2)$$

We shall use this function throughout this course to express the transmission coefficient of rectangular slits.

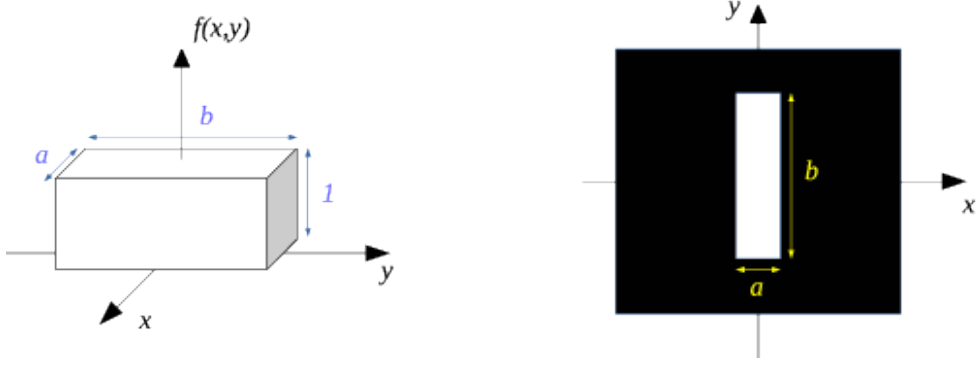


Figure 1: 2D rectangle function $f(x,y) = \Pi\left(\frac{x}{a}\right) \Pi\left(\frac{y}{b}\right)$ of width a in the x direction and b in the y . Left: perspective plot as a function of x and y . Right: gray-level representation in the (x,y) plane.

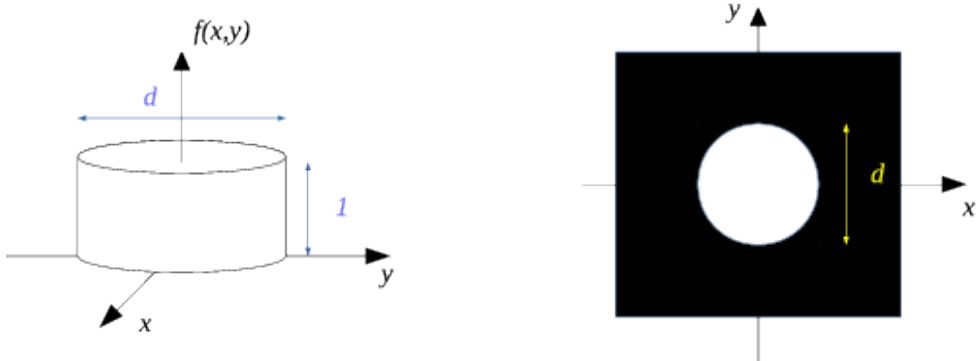


Figure 2: 2D circular function $f(x,y) = \Pi\left(\frac{\rho}{d}\right)$ of diameter d . Left: perspective plot as a function of x and y . Right: gray-level representation in the (x,y) plane.

2D circular function

We consider the following quantity:

$$f(x,y) = \Pi\left(\frac{\rho}{d}\right) \quad (3)$$

with $\rho = \sqrt{x^2 + y^2}$. Its value is one for $\rho < \frac{d}{2}$, i.e. inside a disc of diameter d . This function will be used to describe transmission coefficient of circular diaphragms.

0.1.2 Dirac delta distribution

The Dirac delta distribution (also known as “Dirac impulse”) $\delta(x)$ can be defined as a function which is 0 if $x \neq 0$ and infinite for $x = 0$. Its integral is 1:

$$\int_{-\infty}^{\infty} \delta(x) dx = 1 \quad (4)$$

and this last relation shows that $\delta(x)$ has the dimension of $[x]^{-1}$. The δ distribution is often represented as a vertical arrow centered as $x = 0$, of height 1, as in the graph on the right.

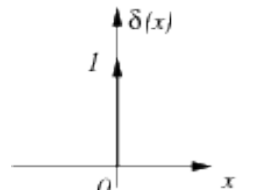
The Dirac δ is sometimes defined as the limit of a rectangular function of width $\epsilon \rightarrow 0$ and height $\frac{1}{\epsilon}$ so that its integral remains 1:

$$\delta(x) = \lim_{\epsilon \rightarrow 0} \frac{1}{\epsilon} \Pi\left(\frac{x}{\epsilon}\right) \quad (5)$$

An important property is:

$$f(x) \delta(x - a) = f(a) \delta(x - a) \quad (6)$$

where $\delta(x - a)$ is the Dirac impulse centered at $x = a$. Some other properties are:



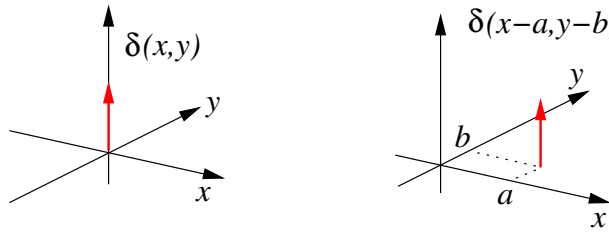


Figure 3: Graphic representation of the 2D Dirac impulses. Left: $\delta(x,y)$. Right: shifted impulse $\delta(x - a, y - b)$ centered at $x = a$, $y = b$.

- $\delta(ax) = \frac{1}{|a|} \delta(x)$ (for $x \neq 0$)
- $\delta(x) = \frac{d}{dx} H(x)$ where $H(x)$ is the Heaviside distribution (1 if $x > 0$, 0 if $x < 0$).

2D Dirac impulse

We define the 2D Dirac distribution as

$$\delta(x, y) = \delta(x) \cdot \delta(y) \quad (7)$$

It is 0 in the whole plane (x, y) excepted at the origin where it is infinite. Its integral is 1:

$$\iint_{-\infty}^{\infty} \delta(x, y) dx dy = 1 \quad (8)$$

The 2D Dirac impulse can be considered as the limit of a rectangular function of width ϵ in both directions x and y (the surface of the rectangle being ϵ^2):

$$\delta(x, y) = \lim_{\epsilon \rightarrow 0} \frac{1}{\epsilon^2} \Pi\left(\frac{x}{\epsilon}\right) \Pi\left(\frac{y}{\epsilon}\right) \quad (9)$$

It is also the limit of a 2D circular function of diameter ϵ (and of surface $s = \pi \frac{\epsilon^2}{4}$)

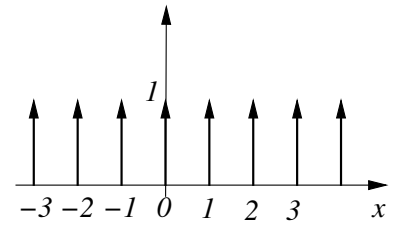
$$\delta(x, y) = \lim_{\epsilon \rightarrow 0} \frac{1}{s} \Pi\left(\frac{\rho}{\epsilon}\right) \quad (10)$$

The 2D Dirac distribution is often used in optics to describe the amplitude of a point-source, or the transmission coefficient of a pin-hole (diaphragm with very small diameter).

0.1.3 Dirac comb

The Dirac comb is a periodic succession of Dirac impulses:

$$\text{III}(x) = \sum_{n=-\infty}^{\infty} \delta(x - n) \quad (11)$$



its period is 1 in the standart form above, its graph (on the right) looks like a comb, hence its name.

It is possible to define a comb of period a , having all δ impulses located at $x = na$ (n integer) as

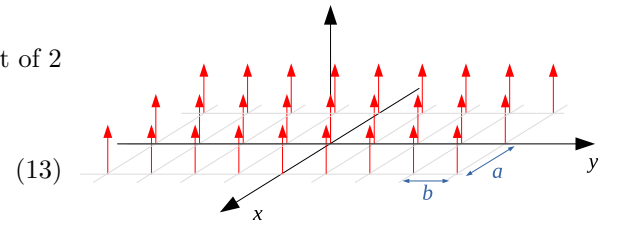
$${}_{a}^{\text{III}}(x) = \sum_{n=-\infty}^{\infty} \delta(x - na) = \frac{1}{|a|} \text{III}\left(\frac{x}{a}\right) \quad (12)$$

The comb is of fundamental importance in signal processing: it is the tool used to describe mathematically the operation of sampling. In optics it is used to describe periodic structures such as diffraction gratings.

2D Dirac comb

The 2D Dirac comb (sometimes denoted as “Dirac brush”) is the product of 2 combs in directions x and y :

$$\text{III}_a(x) \cdot \text{III}_b(y) = \sum_{n=-\infty}^{\infty} \sum_{p=-\infty}^{\infty} \delta(x - na, y - pb)$$



with a and b the periods in x and y directions.

0.2 Convolution

0.2.1 Definition

The convolution product of two functions f and g is defined as

$$h(x) = (f * g)(x) = \int_{-\infty}^{\infty} f(x')g(x - x')dx' \quad (14)$$

It can be interpreted as a weighted moving average of the function f ($g(-x)$ being the weighting function). In signal processing, g is denoted as “impulse response”. If g is a function such as a Gaussian or a rectangle, the convolution will result into a smoothing of the details of f .

2D convolution

The 2D convolution between two functions of (x, y) is

$$h(x, y) = (f * g)(x, y) = \iint_{-\infty}^{\infty} f(x', y')g(x - x', y - y')dx' dy' \quad (15)$$

Note that we use the same symbol $*$ for 1D and 2D convolutions, but the two operations are different (single integral for 1D, double integral for 2D). The 2D impulse response is sometimes denoted as “point-spread function”. The 2D convolution has a lot of applications in image processing; for example convolving an image $f(x, y)$ by a 2D rectangle function will blur the image.

0.2.2 Properties

Here are some properties of the convolution:

- It is commutative ($f * g = g * f$) and associative ($f * (g * h) = (f * g) * h$)
- The convolution by $\mathbf{1}$ gives the integral of the function: $f(x) * \mathbf{1}(x) = \int f(x)dx$ (this can be useful for certain types of calculations).
- Dilatation: $(f * g)(\lambda x) = |\lambda|f(\lambda x) * g(\lambda x)$
- Convoluting by $\delta(x)$ has no effect ($f(x) * \delta(x) = f(x)$). This property is the origin of the term “impulse response” for g in the relation $(f * g)$.
- Convoluting by a shifted impulse $\delta(x - a)$ translates the function: $f(x) * \delta(x - a) = f(x - a)$. This property is very important and useful for Fourier optics calculations.
- Convolution by a comb:

$$f(x) * \text{III}_a(x) = \sum_{n=-\infty}^{\infty} f(x - na) \quad (16)$$

this is a *periodization* of the function f (each impulse of the comb is replaced by f , see Fig. 4).

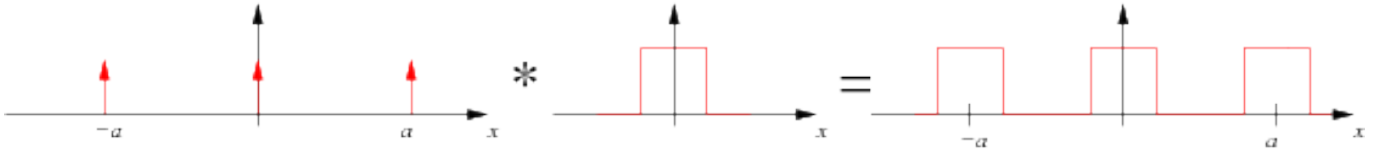


Figure 4: The convolution of a function f by a comb results into a periodization of f (Eq 16). Left, the comb of period a . Center: the function f (here a rectangular function). Right: result of the convolution.

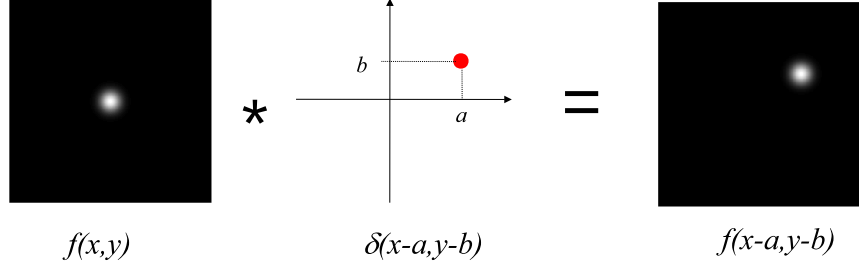


Figure 5: Property of translation of the convolution (Eq. 17): a function $f(x, y)$ (on the left) centered at the origin is convolved by a Dirac impulse centered at $(x = a, y = b)$. The result (on the right) is the shifted function $f(x - a, y - b)$ centered at $(x = a, y = b)$.

2D convolution

Most of the above properties apply to 2D convolution. In particular this one:

$$f(x, y) * \delta(x - a, y - b) = f(x - a, y - b) \quad (17)$$

which is illustrated by the Figure 5. A translation of a function inside the (x, y) plane can be expressed as a convolution by a shifted 2D Dirac impulse. This is the origin of the name “point-spread function” (PSF) for the impulse response at 2D (a 2D Dirac impulse is a infinitely sharp point in the (x, y) plane, and the convolution transforms this point into a larger function f).

A corollary of this property is:

$$f(x, y) * \sum_n A_n \delta(x - x_n, y - y_n) = \sum_n A_n f(x - x_n, y - y_n) \quad (18)$$

which is illustrated by Figs. 6 and 7.

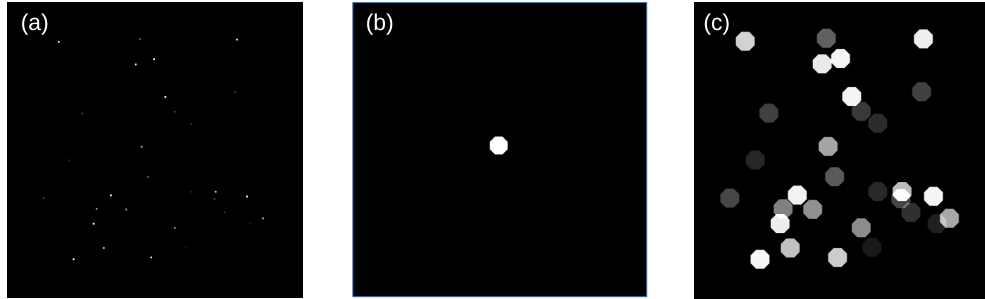


Figure 6: Illustration of Eq. 18. (a) gray-scale plot of a sum of 2D Dirac impulses with different amplitudes. (b) gray-scale plot of the point-spread function $f(x, y)$ ($f(x, y) = 1$ inside an octagonal domain, 0 elsewhere). (c) result of the 2D convolution of the two functions. As predicted by Eq. 18, the result is a sum of shifted PSFs (each impulse of the sum is replaced by the PSF, with the same amplitude A_n) When PSFs overlap, the result is the sum of overlapping terms.

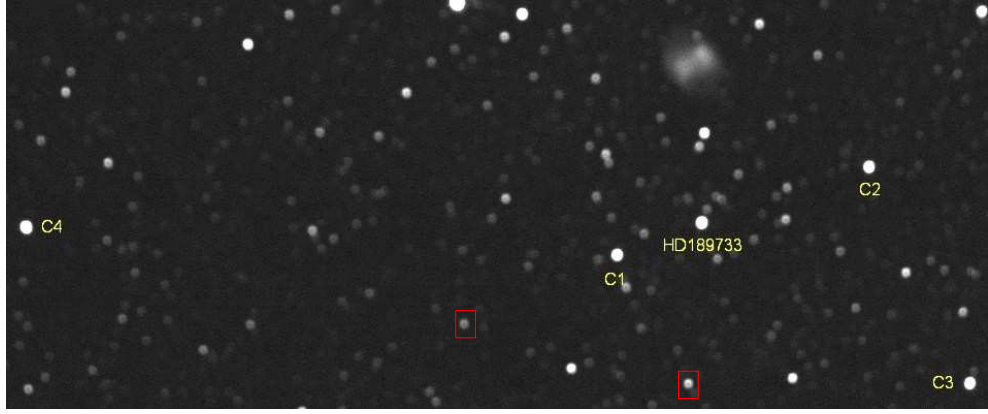


Figure 7: Image of portion of sky with a defocused optics: each star has the shape of a small disc, with a central obstruction. This is a typical illustration of a 2D convolution as in Fig. 7. The perfect image $f(x, y)$ is composed of a sum of 2D impulses (ideal image of a point-source). It is convolved by a Point-Spread function $g(x, y)$ which is the small disc (two examples are in the red boxes). The fuzzy object on the top right is the Dumbbell nebula, which is also convolved by the PSF (so that every point of the nebula is replaced by the PSF, resulting in a blurred image).

0.3 Fourier transform

0.3.1 Definition

The Fourier transform of a function $f(x)$ is defined as

$$\hat{f}(u) = \int_{-\infty}^{\infty} f(x) e^{-2i\pi ux} dx \quad (19)$$

it can be noted as $\hat{f}(u)$ or $\mathcal{F}[f]$. It is sometimes denoted as *frequency spectrum*, since it comes from the idea that a function can be developed as a weighted sum of complex sinusoids. The value $\hat{f}(u)$ represents the weight of the sinusoid of frequency u in the sum.

If x is a length, the variable u is a spatial frequency, having the dimension of $[x]^{-1}$. The spatial frequency of a space-dependent sinusoidal function (for ex. $\cos(2\pi u x)$) plays the same role as the temporal frequency for a time-dependent function, it represents the number of periods per unit of length. The dimension of $\hat{f}(u)$ is

$$[\hat{f}(u)] = [f].[x] \quad (20)$$

A very important property is

$$\mathcal{F}[\exp(2i\pi u_0 x)] = \delta(u - u_0) \quad (21)$$

i.e. the Fourier transform of a complex sinusoid of frequency u_0 is a Dirac impulse centered at u_0 . This emphasizes the fact that the complex sinusoid has only one frequency in its spectrum.

The inverse Fourier transform is

$$f(x) = \int_{-\infty}^{\infty} \hat{f}(u) e^{+2i\pi ux} du = \mathcal{F}^{-1}[\hat{f}] \quad (22)$$

2D Fourier transform

The 2D Fourier transform of a function of two variables $f(x, y)$ is defined as

$$\hat{f}(u, v) = \iint_{-\infty}^{\infty} f(x, y) e^{-2i\pi(ux+vy)} dx dy \quad (23)$$

The variables u and v are spatial frequencies associated to the space variables x and y . They define, in the (u, v) plane, a “spatial frequency vector” $\vec{\sigma} = \begin{pmatrix} u \\ v \end{pmatrix}$ (see Fig. 8). As for the 1D Fourier transform, the idea is that a function $f(x, y)$ can be expressed as a sum of 2D complex sinusoids of any period and any orientation.

The 2D inverse Fourier transform is

$$f(x, y) = \iint_{-\infty}^{\infty} \hat{f}(u, v) e^{+2i\pi(ux+vy)} dx dy \quad (24)$$

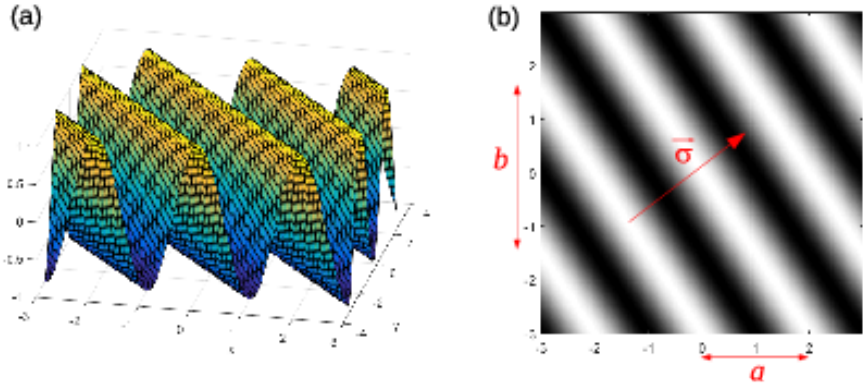


Figure 8: Representation of a 2D sinusoidal function $f(x, y) = \cos(2\pi\vec{\sigma} \cdot \vec{\rho}) = \cos(2\pi(ux + vy))$. (a): perspective plot. (b): grayscale plot. The frequency vector $\vec{\sigma} = (u, v)$ has been drawn on the right plot; it is perpendicular to the ridge lines of the function, its modulus is the frequency of the oscillations measured along the unit vector $\hat{\sigma}$. Its components are $u = \frac{1}{a}, v = \frac{1}{b}$ with a and b the periods in the x and y directions.

0.3.2 Properties

Here is a short list of useful properties of the 1D Fourier transform

- Dilatation: a function which is large in the direct plane will be narrow in the Fourier plane

$$f\left(\frac{x}{a}\right) \xrightarrow{\mathcal{F}} |a| \hat{f}(au) \quad (25)$$

- Convolution and product:

$$\begin{aligned} f(x) \cdot g(x) &\xrightarrow{\mathcal{F}} \hat{f}(u) * \hat{g}(u) \\ f(x) * g(x) &\xrightarrow{\mathcal{F}} \hat{f}(u) \cdot \hat{g}(u) \end{aligned} \quad (26)$$

- Derivation: the Fourier transform of the derivative of a function is a high-pass filtering in the frequency plane (product by u which strengthens the high frequencies)

$$\begin{aligned} \frac{df}{dx} &\xrightarrow{\mathcal{F}} 2i\pi u \hat{f}(u) \\ x \cdot f(x) &\xrightarrow{\mathcal{F}} -\frac{1}{2i\pi} \frac{d\hat{f}}{du} \end{aligned} \quad (27)$$

- Value at frequency $u = 0$: it is the integral of the function (this property is sometimes interesting to calculate integrals)

$$\hat{f}(0) = \int_{-\infty}^{\infty} f(x) dx \quad (28)$$

- Sign change for the variable x :

$$f(-x) \xrightarrow{\mathcal{F}} \hat{f}(-u) \quad (29)$$

- Complex conjugate:

$$\overline{f(x)} \xrightarrow{\mathcal{F}} \overline{\hat{f}(-u)} \quad (30)$$

- Double Fourier transform:

$$f(x) \xrightarrow{\mathcal{F}} \hat{f}(u) \xrightarrow{\mathcal{F}} f(-x) \quad (\text{or: } \hat{f}(x) = f(-x)) \quad (31)$$

- Fourier transform of real-valued functions: they are *Hermitian*, with an even real part and an odd imaginary part. It can be summarized by

$$\text{is } f(x) \text{ real , then } \overline{\hat{f}(u)} = \hat{f}(-u) \quad (32)$$

- Real/even functions: if a function f is real and even, then
 - Its Fourier transform is also real and even (no imaginary part)
 - Its inverse transform is equal to its direct transform: $\mathcal{F}^{-1}[f](u) = \mathcal{F}[f](u)$
- Parseval theorem:

$$\int_{-\infty}^{\infty} |\hat{f}(x)|^2 dx = \int_{-\infty}^{\infty} |\hat{f}(u)|^2 du \quad (33)$$

Specific properties for 2D Fourier transform

Separable functions: if a function $h(x, y)$ is the product of two functions of one variable $f(x)$ and $g(y)$, then its 2D Fourier transform is also a separable function, i.e.

$$h(x, y) = f(x) \cdot g(y) \xrightarrow{\mathcal{F}} \hat{h}(u, v) = \hat{f}(u) \cdot \hat{g}(v) \quad (34)$$

This property must not to be confused with the Fourier transform of a product of functions of the same variables (Eq. 26): here the variables for f and g are different, and the 2D transform is a double integral.

Radial functions of the type $f(x, y) = f(\rho)$ with $\rho = \sqrt{x^2 + y^2}$: the 2D Fourier transform $\hat{f}(u, v)$ is also a radial function $F(q)$ with $q = \sqrt{u^2 + v^2}$. It takes the following form known as *Hankel transform*:

$$F(q) = \hat{f}(u, v) = \int_0^{\infty} 2\pi\rho f(\rho) J_0(2\pi q\rho) d\rho \quad (35)$$

where $J_0(x)$ is the zero order Bessel function. The Hankel transform $f(\rho) \rightarrow F(q)$ is not to be confused with the 1D Fourier transform (Eq. 19).

0.3.3 Table of Fourier transforms

1D transforms

Function	Fourier transform	Function	Fourier transform
$\delta(x)$	$\mathbf{1}(u)$	$\mathbf{1}(x)$	$\delta(u)$
$\delta(x - a)$	$\exp(-2i\pi ua)$	$\exp(2i\pi mx)$	$\delta(u - m)$
Heaviside $H(x)$ <i>H(x) = 1 if x > 0, 0 otherwise</i>	$\frac{1}{2}\delta(u) + \text{VP} \left(\frac{1}{2i\pi u} \right)$	$\Pi \left(\frac{x}{a} \right)$	$ a \text{sinc}(\pi ua)$ with $\text{sinc}(x) = \frac{\sin(x)}{x}$
$\text{III}_a(t)$	$\text{III}(au)$	Triangle $\Lambda \left(\frac{x}{a} \right)$ <i>$\Lambda(x) = 1 - x$ if $x \leq 1$, 0 otherwise</i>	$ a \text{sinc}^2(\pi ua)$
$\cos(2\pi mx)$	$\frac{1}{2}\delta(u - m) + \frac{1}{2}\delta(u + m)$	$\sin(2\pi mx)$	$-\frac{1}{2}\delta(u - m) + \frac{1}{2}\delta(u + m)$
$\exp \left(-\left \frac{x}{a} \right \right)$	$\frac{2 a }{1 + 4\pi^2 a^2 u^2}$	$\frac{1}{1 + \left(\frac{x}{a} \right)^2}$	$\pi a \exp(-2\pi au)$
$\exp \left[-\pi \left(\frac{x}{a} \right)^2 \right]$	$ a \exp(-\pi a^2 u^2)$	$\exp \left[i\pi \left(\frac{x}{a} \right)^2 \right]$	$\sqrt{ia^2} \exp(-i\pi a^2 u^2)$

2D transforms (radial functions)

Function	Fourier transform	Function	Fourier transform
$\delta(\rho - a)$	$2\pi a J_0(2\pi aq)$	$\frac{1}{\sqrt{\rho^2 + a^2}}$	$\frac{\exp(-2\pi aq)}{q}$
$\Pi \left(\frac{\rho}{d} \right)$ <i>$\text{jinc}(x) = \frac{J_1(x)}{x}$</i> <i>$S = \frac{\pi d^2}{4}$</i>	$2S \text{jinc}(\pi dq)$	$\text{大} \left(\frac{\rho}{d} \right)$ <i>$\text{大}(\rho) = \Pi(\rho) * \Pi(\rho)$</i>	$4S \text{jinc}(\pi dq)^2$
$\exp(-\pi\rho^2)$	$\exp(-\pi q^2)$	$\exp \left(i\pi \frac{\rho^2}{a^2} \right)$	$ia^2 \exp(-i\pi a^2 q^2)$

with $\rho = \sqrt{x^2 + y^2}$ and $q = \sqrt{u^2 + v^2}$

Chapter 1

Reminders about diffraction

Also read : Goodman, ‘Introduction to Fourier Optics’, chap. 3, 4

1.1 Some particular kinds of waves

1.1.1 Monochromatic waves

Electromagnetic waves are created by the propagation of an electromagnetic field (\vec{E}, \vec{B}). Both are vectorial quantities, but the majority of diffraction phenomena can be explained by considering the scalar quantity $E(x, y, z, t)$ (either the electric or magnetic field, without vectors).

A monochromatic wave is characterised by a time dependence in $e^{-i\omega t}$. It has only **one pulsation** ω (with $\omega = 2\pi\nu$ where ν is the temporal frequency, typically 10^{15} Hz for visible light). It also has a unique wavelength $\lambda = \frac{c}{\nu}$ (or $\lambda = \frac{c}{n\nu}$ if the refraction index is n) whose dimension is a length (in m).

The field $E(x, y, z, t)$ takes the following form of a product of a spatial term and a temporal term:

$$E(x, y, z, t) = \psi(x, y, z) e^{-i\omega t} \quad (1.1)$$

where $\psi(x, y, z)$ (or $\psi(\vec{r})$), the spatial part of the field, is called the *complex amplitude* of the vibration. In what follows we will consider that all the waves are monochromatic, and will deal with complex amplitudes.

1.1.2 Plane waves

Wavefronts (i.e. surfaces where the electric field value is constant at a given time) are planes. The distance between two consecutive wavefronts is the wavelength λ (two consecutive wavefronts are characterized by a 2π phase difference between complex amplitudes in both planes).

We define the wave vector $\vec{k} = \frac{2\pi}{\lambda} \hat{k}$. Its norm is $\frac{2\pi}{\lambda}$ and its unit vector \hat{k} is parallel to the direction of propagation (see Fig. 1.1).

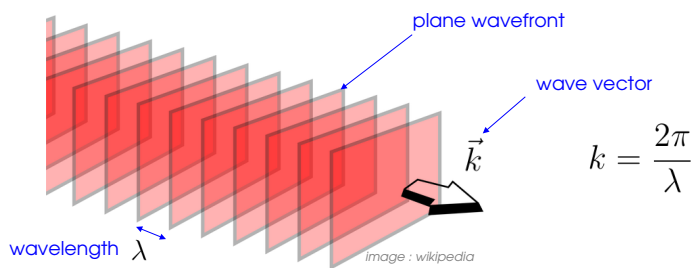


Figure 1.1: Structure of a plane wave

The electric field \vec{E} of a monochromatic plane wave takes the form

$$\vec{E} = \psi_0 e^{i(\vec{k} \cdot \vec{r} - \omega t)} \hat{E} \quad (1.2)$$

with ψ_0 a constant [unit: V/m] and \hat{E} a unit vector, perpendicular to \vec{k} . Note that \vec{E} is constant in a plane perpendicular to \vec{k} (i.e. wave planes are perpendicular to \vec{k} , see Fig. 1.1).

We denote as α , β and γ the three components of the unit vector \hat{k} (projections of \hat{k} onto the 3 axes as in the scheme on the right). The wave vector expresses as

$$\vec{k} = \frac{2\pi}{\lambda} (\alpha \hat{x} + \beta \hat{y} + \gamma \hat{z}) \quad (1.3)$$

with the condition $\sqrt{\alpha^2 + \beta^2 + \gamma^2} = 1$ (\hat{k} is a unit vector).

The case ($\alpha = \beta = 0, \gamma = 1$) corresponds to a propagation parallel to the z axis.

With these notations, the complex amplitude of a monochromatic plane wave takes the form

$$\psi(\vec{r}) = \psi_0 e^{i\vec{k} \cdot \vec{r}} = \psi_0 \exp \left[\frac{2i\pi}{\lambda} (\alpha x + \beta y + \gamma z) \right] \quad (1.4)$$

It exhibits a phase term which is a linear function of coordinates (x, y, z) .

Intensity It is the electromagnetic power per surface unit carried by the electromagnetic wave. It is proportional to the square modulus of the complex amplitude

$$I = (C^{te}) |\psi(\vec{r})|^2 \quad (1.5)$$

the multiplicative constant is generally taken as unity for a sake of simplicity.

1.1.3 Spherical waves

Wavefronts are concentric spheres (Fig. 1.2). If the center of these spheres is at the point $(0, 0, 0)$, the complex amplitude expresses as

$$\psi(\vec{r}) = \frac{S_0}{r} e^{ik.r} \quad \text{or} \quad \psi(\vec{r}) = \frac{S_0}{r} e^{-ik.r} \quad (1.6)$$

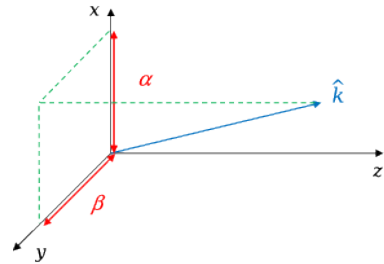
without vectors in the complex exponential. The sign + (resp. -) denotes a diverging (resp. converging) spherical wave: the radius of the wave-spheres increase (resp decrease) with time. Note that

- The point $r = 0$ (center of the spheres) is singular, the field value diverges. It can be a *point-source* (case of a diverging wave) or a point of focalisation (converging wave).
- The dimension of S_0 is *not* that of an amplitude ($[S_0] = [\psi].[r]$, in V).

Case of a spherical wave not centered at the origin: if we call $\vec{r}_0 = (x_0, y_0, z_0)$ the center of wave-spheres, a simple translation allows to write the complex amplitude as:

$$\psi(\vec{r}) = \frac{S_0}{|\vec{r} - \vec{r}_0|} e^{\pm ik \cdot |\vec{r} - \vec{r}_0|} \quad (1.7)$$

with $|\vec{r} - \vec{r}_0| = \sqrt{(x - x_0)^2 + (y - y_0)^2 + (z - z_0)^2}$.



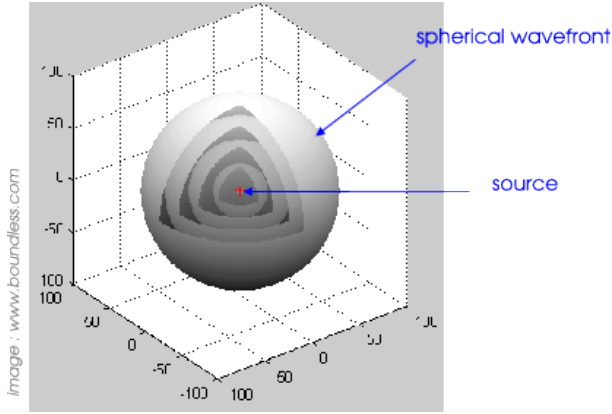
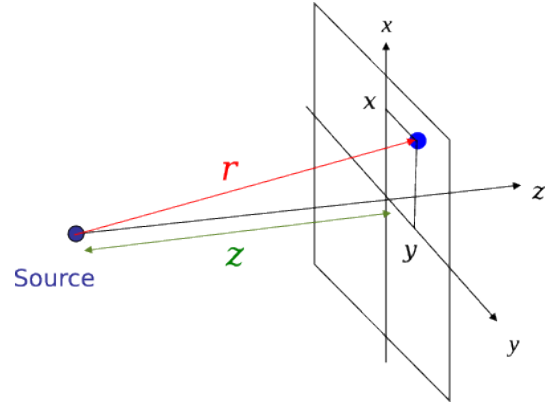


Figure 1.2: Structure of a spherical wave.

Paraxial approximation

It is an important approximation in Fourier optics, the majority of relations will be derived within this approximation. We consider that the segment joining the source and the point at \vec{r} is nearly parallel to the z -axis, as illustrated by the scheme on the right. If the source is at the origin, we have $|x| \ll |z|$ and $|y| \ll |z|$, and make the following approximation for r :

$$r \simeq |z| + \frac{\rho^2}{2|z|} \quad \text{with} \quad \rho^2 = x^2 + y^2 \quad (1.8)$$



The complex amplitude in paraxial approximation (if the source is at the origin) becomes

$$\psi(\vec{r}) \simeq \underbrace{\frac{S_0}{|z|} e^{\pm ik|z|}}_{\text{plane wave}} \cdot \underbrace{\exp\left(\pm \frac{i\pi\rho^2}{\lambda|z|}\right)}_{\text{phase curvature}} \quad (1.9)$$

It is the product of two terms

- A plane wave $\frac{S_0}{|z|} e^{\pm ik|z|}$ with wave-planes perpendicular to z ,
- A quadratic phase term $\exp\left(\pm \frac{i\pi\rho^2}{\lambda|z|}\right)$ which can be interpreted as a deviation from the plane wave. The wavefronts associated to this term are paraboloids (a paraboloid is indeed the 2nd order approximation of a sphere). This term is sometimes denoted as *phase curvature* because it is a pure phase term and in reference to the curvature of the wavefronts (see Fig. 1.3).

Plots of the paraxial form of the spherical wave amplitude are shown in Fig. 1.4. In a plane $z = C^{te}$, it is a centro-symmetric function whose real and imaginary part show concentric rings of characteristic size $\sqrt{\lambda z}$ (for $z > 0$).

For large z , the phase curvature vanishes and the spherical wave becomes plane. This happens when $|z| \gg \rho^2/\lambda$ (1m for $\lambda = 1\mu\text{m}$ and $\rho = 1\text{mm}$).

Validity of the approximation

The approximate expression for r in Eq. 1.8 is the leading terms of a Taylor expansion. The approximation is valid if the following term is small:

$$r \simeq |z| + \frac{\rho^2}{2|z|} + \frac{\rho^4}{8|z|^3} + \dots \quad (1.10)$$

The corresponding complex amplitude is

$$\psi(\vec{r}) \simeq \frac{S_0}{|z|} e^{\pm ik|z|} \exp\left(\pm \frac{i\pi\rho^2}{\lambda|z|}\right) \exp\left(\pm \frac{i\pi\rho^4}{4\lambda|z|^3}\right) \quad (1.11)$$

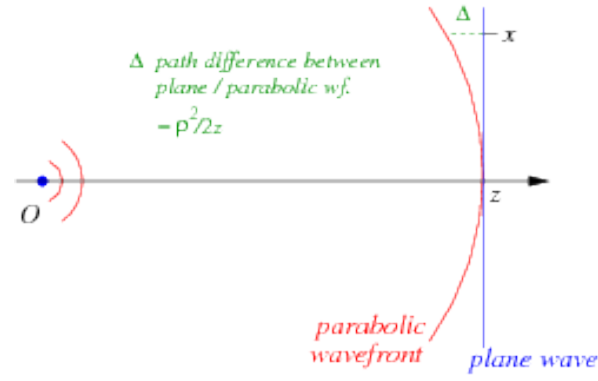


Figure 1.3: Paraxial approximation of a spherical wave, in the case of $z \gg \rho$. In this example, z is positive and the wave is diverging (+ sign in the complex exponentials). The spherical wave is the product of a plane wave under normal incidence (blue wave-plane) and a correcting term (phase curvature $e^{ik\Delta}$, red wavefront) as written in Eq. 1.9. The quantity $\Delta = \frac{\rho^2}{2z}$ is the path difference between blue and red wavefronts.

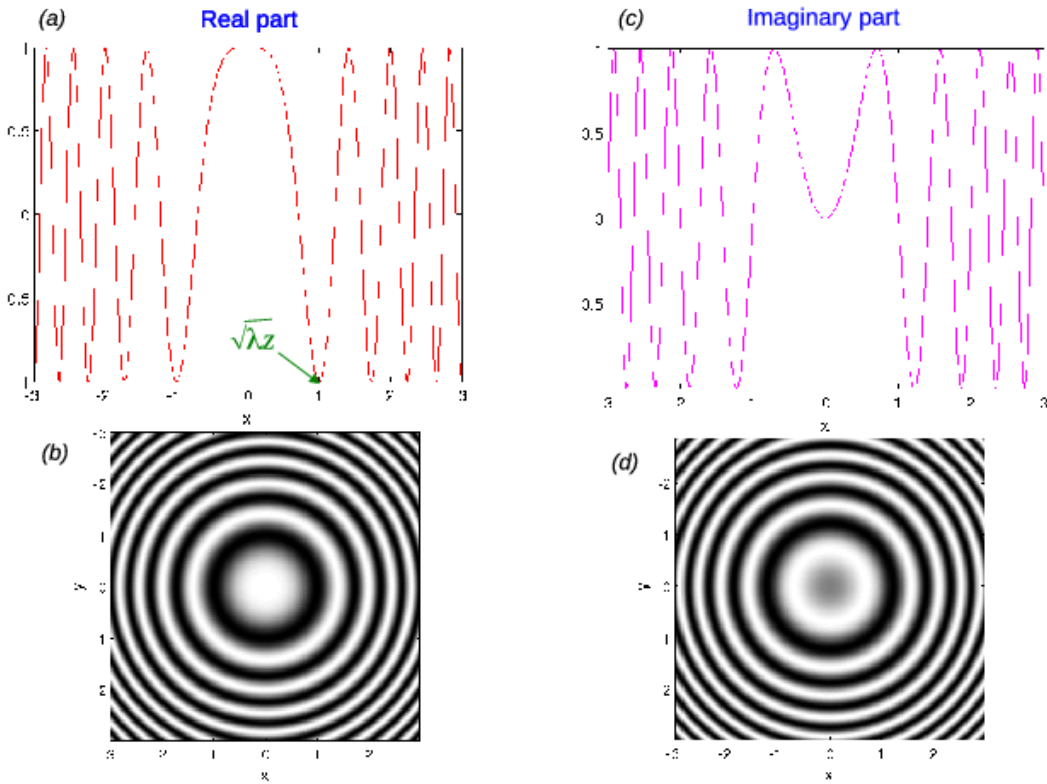


Figure 1.4: Plot of the complex amplitude $\psi(x, y, z) = C^{te} \exp\left(\frac{i\pi\rho^2}{\lambda z}\right)$ of a spherical wave in paraxial approximation for fixed z . (a) and (c): Real and imaginary parts as a function of ρ (in units of $\sqrt{\lambda z}$). (b) and (d): Grey-level plot of the real and imaginary parts in the (x, y) plane.

The paraxial approximation (Eq. 1.9) is valid if the last term is close to unity, i.e. if

$$|z| \gg \left(\frac{\rho^4}{\lambda} \right)^{\frac{1}{3}} \quad (1.12)$$

In visible light ($\lambda = 0.5\mu\text{m}$) and for $\rho=1\text{mm}$ this gives a few centimeters.

Case of a source at a position $\vec{r}_0 = (x_0, y_0, z_0)$: Making the variable change $x \rightarrow x - x_0$, $y \rightarrow y - y_0$, $z \rightarrow z - z_0$, we obtain

$$\psi(\vec{r}) \simeq \frac{S_0}{|z - z_0|} e^{\pm ik|z - z_0|} \exp \left(\pm \frac{i\pi[(x - x_0)^2 + (y - y_0)^2]}{\lambda|z - z_0|} \right) \quad (1.13)$$

1.2 Huyghens-Fresnel principle

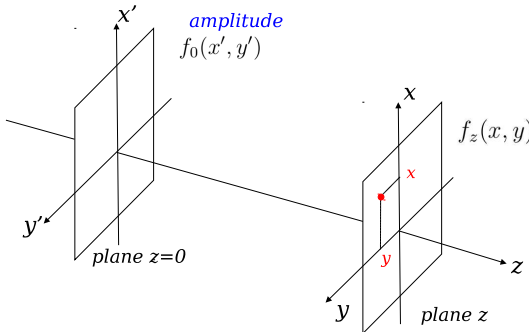
Also read : Goodman, "Introduction to Fourier Optics", chap 4.

1.2.1 Introduction

The Huygens-Fresnel principle describes the way a monochromatic wave is modified when it propagates into space (this phenomenon is called *diffraction*). We shall consider a monochromatic wave of amplitude $f_0(x', y')$ in a plane taken as origin, $z = 0$. This can be obtained, for example, by placing a screen of transmission $t(x', y')$ (for example a slit or a diaphragm) in the path of a monochromatic plane wave of complex amplitude $\mathcal{A} = Ae^{ikz}$. In this case we simply have

$$f_0(x', y') = A t(x', y') \quad (1.14)$$

The observation is made at in a plane a distance z from the plane $z = 0$, as in the scheme below. Note that we use the notations (x', y') for coordinates in the plane $z = 0$ and (x, y) in the observation plane. We suppose that the propagation is made towards $z > 0$, which will be assumed for the rest of this course.



In the observation plane at a point P of coordinates (x, y, z) , we denote as $f_z(x, y)$ the complex amplitude. This notation emphasises the fact that is is a 2D structure in x and y , and that z is here a parameter. The Huygens-Fresnel principle show that $f_z(x, y)$ expresses as a sum of complex amplitudes produced by all the points of $f_0(x', y')$

$$f_z(x, y) = \frac{e^{ikz}}{i\lambda} \iint_{-\infty}^{\infty} f_0(x', y') \frac{\exp(i k |\vec{r} - \vec{r}'|)}{|\vec{r} - \vec{r}'|} dx' dy' \quad (1.15)$$

where $\vec{r} = (x, y, z)$ and $\vec{r}' = (x', y', 0)$. This integral is indeed a continuous sum of spherical waves centered at every point \vec{r}' on the plane $z = 0$ (Huyghens wavelets).

1.2.2 Paraxial approximation and Fresnel diffraction

When the paraxial approximation is valid, the above integral becomes

$$f_z(x, y) = \frac{e^{ikz}}{i\lambda z} \iint_{-\infty}^{\infty} f_0(x', y') \exp \left(i\pi \frac{(x - x')^2 + (y - y')^2}{\lambda z} \right) dx' dy' \quad (1.16)$$

This paraxial form of the Huyghens-Fresnel principle is known as *Fresnel diffraction* and is valid for $z \gg \left(\frac{d^4}{\lambda} \right)^{\frac{1}{3}}$ with d the size of the diffracting aperture (width of the function $f_0(x', y')$).

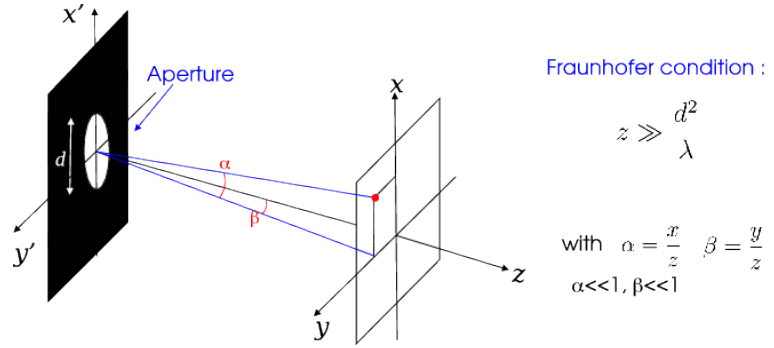


Figure 1.5: Geometry for the Fraunhofer diffraction by an aperture in the plane $z = 0$. x and y are coordinates in the observation plane at large distance z from aperture plane. d is here the aperture diameter.

The equation 1.16 is a convolution relation, which we can note as:

$$f_z(x, y) = e^{ikz} f(x, y) * D_z(x, y) \quad (1.17)$$

where the term e^{ikz} expresses the propagation of a plane wave on the distance z , and

$$D_z(x, y) = \frac{1}{i\lambda z} \exp\left(i\pi \frac{\rho^2}{\lambda z}\right) \quad \text{with } \rho^2 = x^2 + y^2$$

is the complex amplitude of a spherical wave of center O . This convolution relation expresses $f_z(x, y)$ as the sum of spherical waves produced by point-sources in the plane $z = 0$.

The function D_z is the “amplitude point-spread function” of the Fresnel diffraction. It is a normalized function:

$$\iint_{-\infty}^{\infty} D_z(x, y) dx dy = 1$$

1.2.3 Far field: Fraunhofer diffraction

Fraunhofer diffraction (or diffraction at infinity) is the limit of the Fresnel diffraction when the distance z tends towards infinity (far-field hypothesis). The equation (1.16) writes as:

$$f_z(x, y) = \frac{e^{ikz}}{i\lambda z} \iint_{-\infty}^{\infty} f_0(x', y') \exp\left(\frac{i\pi z}{\lambda} \left[\frac{\rho^2}{z^2} + \frac{\rho'^2}{z^2} - 2\frac{xx' + yy'}{z^2} \right]\right) dx' dy' \quad (1.18)$$

with $\rho^2 = x^2 + y^2$ and $\rho'^2 = x'^2 + y'^2$. Since $z \rightarrow \infty$, we assume $\rho \ll z$ and $\rho' \ll z$ and neglect the second order terms in $\frac{\rho^2}{z^2}$ and $\frac{\rho'^2}{z^2}$ in the exponential term. The above equation simplifies in

$$f_z(x, y) = \frac{e^{ikz}}{i\lambda z} \iint_{-\infty}^{\infty} f_0(x', y') \exp\left(-2i\pi \left[x' \frac{x}{\lambda z} + y' \frac{y}{\lambda z} \right]\right) dx' dy' \quad (1.19)$$

We recognise the expression of a Fourier transform

$$f_z(x, y) = \frac{e^{ikz}}{i\lambda z} \hat{f}_0\left(\frac{x}{\lambda z}, \frac{y}{\lambda z}\right)$$

(1.20)

where the symbol $\hat{\cdot}$ stands for the Fourier transform. We can introduce the quantities $\alpha = \frac{x}{z}$ and $\beta = \frac{y}{z}$, which are angular coordinates of a point in the observation plane as seen from the origin (see Fig. 1.5). We obtain the angular form of the Fraunhofer diffraction formula:

$$f_z(\alpha, \beta) = \frac{e^{ikz}}{i\lambda z} \hat{f}_0\left(\frac{\alpha}{\lambda}, \frac{\beta}{\lambda}\right) \quad (1.21)$$

In the direction α and β , the diffracted amplitude is proportional to the Fourier transform of the screen. The intensity is thus proportional to the power spectrum of $f(x, y)$, i.e. $\left|\hat{f}_0\left(\frac{\alpha}{\lambda}, \frac{\beta}{\lambda}\right)\right|^2$.

This kind of calculation is often met in the field of signal processing; it is possible to use the phenomenon of Fraunhofer diffraction to realise the 2-dimensional Fourier transform. Experimentally, Fraunhofer conditions can be obtained by diffraction on a distance of several meters or tens of meters. Such an optical setup is somewhat cumbersome and needs a very bright light source (f_z is proportional to $1/z$). But in next chapter we shall see that the use of a converging lens allow to observe Fraunhofer diffraction at finite distance.

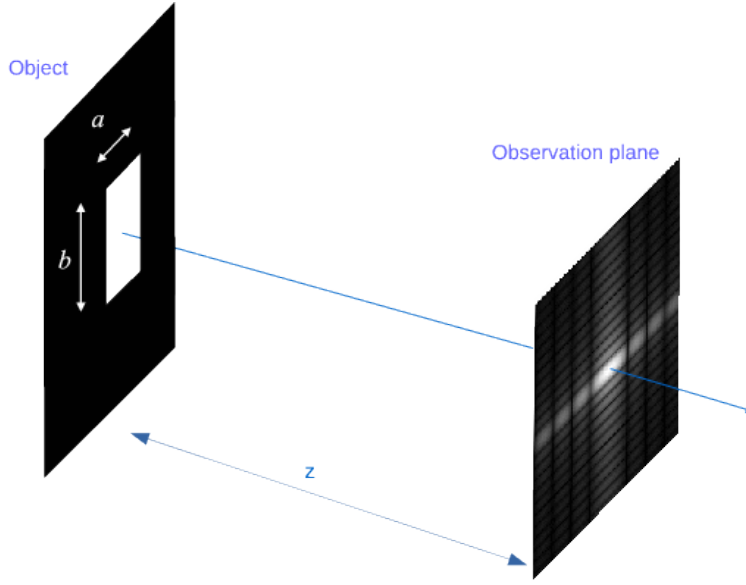


Figure 1.6: Fraunhofer diffraction by a rectangular slit in the plane $z = 0$.

Validity of the approximation

Fraunhofer diffraction is valid if both the terms $\frac{\rho^2}{z^2}$ and $\frac{\rho'^2}{z^2}$ in the exponential term of Eq. 1.18 can be neglected. This exponential term can be developed as:

$$\exp\left(\frac{i\pi z}{\lambda} \left[\frac{\rho^2}{z^2} + \frac{\rho'^2}{z^2} - 2\frac{xx' + yy'}{z^2} \right] \right) = \exp\left(\frac{i\pi\rho^2}{\lambda z}\right) \cdot \exp\left(\frac{i\pi\rho'^2}{\lambda z}\right) \cdot \exp\left(-2i\pi \left[\frac{x'x}{\lambda z} + \frac{y'y}{\lambda z} \right]\right) \quad (1.22)$$

The term in ρ'^2 can be neglected if $\exp\left(\frac{i\pi\rho'^2}{\lambda z}\right) \simeq 1$, thus if $\rho'^2 \ll \lambda z$. If the size of the diffracting aperture is d (so that $\rho' \leq d$ in the integral of Eq. 1.18), we obtain a condition on z to apply Fraunhofer diffraction:

$$z \gg \frac{d^2}{\lambda} \quad (1.23)$$

In the visible domain ($\lambda = 500\text{nm}$), this gives $z > 2\text{m}$ for $d = 1\text{mm}$, and $z > 200\text{m}$ for $d = 1\text{cm}$.

1.2.4 Example of Fraunhofer diffraction patterns

Rectangular slit

The object is a rectangular slit of width a in the x direction and b in the y direction (see Fig. 1.6). Its transmission can be written as

$$t(x, y) = \Pi\left(\frac{x}{a}\right) \Pi\left(\frac{y}{b}\right) \quad (1.24)$$

We suppose that this slit is lit by a plane wave under normal incidence whose amplitude is A in the plane of the slit. Applying Eq. 1.20, the diffracted amplitude at distance z under Fraunhofer approximation is

$$f_z(x, y) = A e^{ikz} \frac{ab}{i\lambda z} \operatorname{sinc}\left(\frac{\pi ax}{\lambda z}\right) \operatorname{sinc}\left(\frac{\pi by}{\lambda z}\right) \quad (1.25)$$

The graph of the corresponding intensity is displayed in Fig. 1.7. It exhibits, in both directions, a central lobe surrounded by secondary maxima. The brightest secondary maximum has an intensity of 4.5% of the maximum. The half-size of the central lobe in the x (resp y) direction is $\lambda z/a$ (resp. $\lambda z/b$), inversely proportional to the slit width. The position of the secondary minima (in the x direction) is periodically distributed at $p\lambda z/a$ ($p \neq 0$).

Circular diaphragm

The object is a circular aperture of diameter a . Its transmission is

$$t(x, y) = \Pi\left(\frac{\rho}{a}\right) \quad \text{with} \quad \rho = \sqrt{x^2 + y^2} \quad (1.26)$$

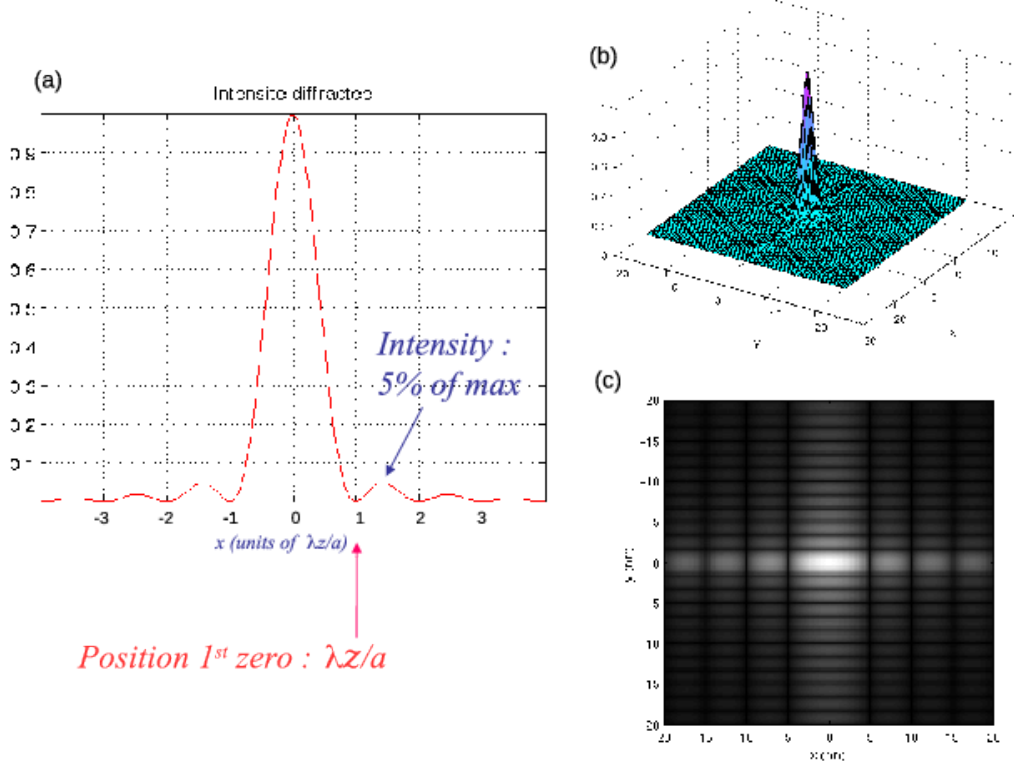


Figure 1.7: Intensity diffracted by a rectangular slit in Fraunhofer approximation. (a) Plot of the normalised intensity as a function of x . (b) Perspective plot of the 2D intensity in the (x, y) plane. (c) Gray level plot showing the aspect of the image.

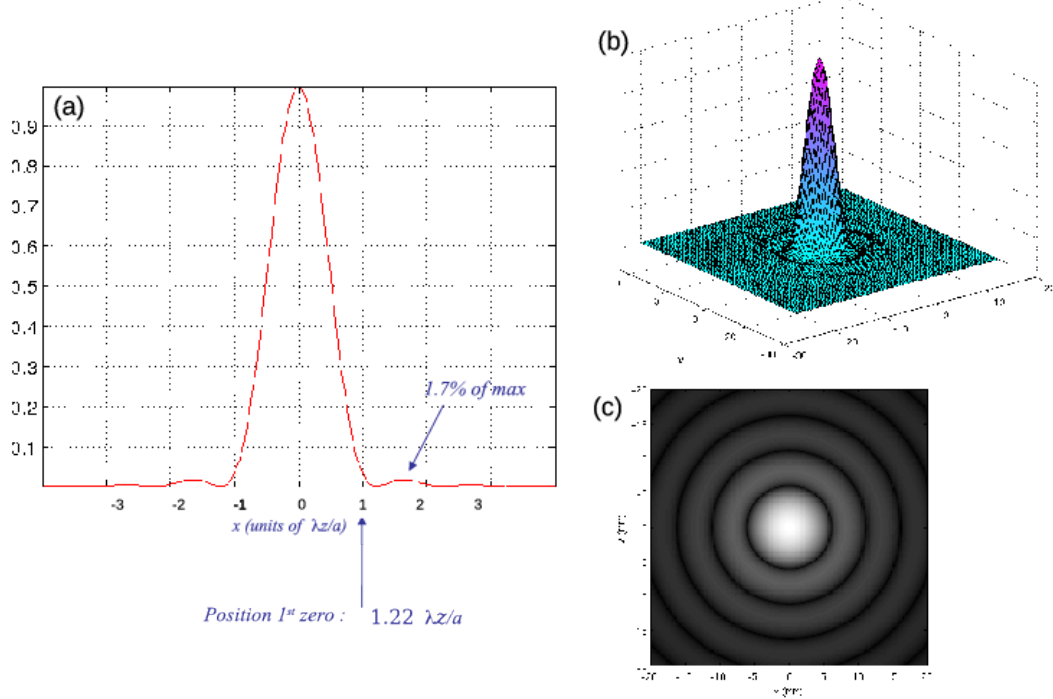


Figure 1.8: Airy disc: intensity diffracted by a circular aperture. (a) Plot of the normalised intensity as a function of x . (b) Perspective plot of the 2D intensity in the (x, y) plane. (c) Gray level plot showing the aspect of the image.

As for the previous example, the incident wave is plane with normal incidence and amplitude A in the aperture plane. Note that the wave in the plane $z = 0$ is invariant by rotation around the z -axis: its diffraction pattern has the same symmetry. The diffracted amplitude at distance z is

$$f_z(x, y) = A e^{ikz} \frac{S}{i\lambda z} 2 \text{jinc} \left(\frac{\pi a \rho}{\lambda z} \right) \quad \text{with} \quad S = \frac{\pi a^2}{4} \quad (\text{aperture surface}) \quad (1.27)$$

which looks very similar to the amplitude diffracted by a slit of same width a , excepted that the sinc function is replaced by a jinc (preceded by a multiplicative factor 2 because $\text{jinc}(0)=\frac{1}{2}$). The intensity is the well-known *Airy* function:

$$I(x, y) = \frac{|A|^2 S^2}{\lambda z} 4 \text{jinc}^2 \left(\frac{\pi a \rho}{\lambda z} \right) \quad (1.28)$$

its graph is displayed in Fig. 1.8. It has the appearance of a bright disc surrounded by faint rings (Airy disc). The radius of the central lobe is $1.22 \lambda z/a$. The first secondary ring has an intensity of 1.7% of the maximum. Note that radii of dark rings is not periodic (as it was the case for the slit).

It is interesting to compare the diffraction patterns (intensity) produced by a disc of diameter a and a square of same side a (Fig. 1.9). Some differences may be noticed:

- the size of the central lobe is larger in the case of the disc (by 22%),
- the central lobe contains more energy in the case of the disc (84% of the integrated intensity for the disc, 81% for the square),
- secondary maxima are fainter for the disc (1st maximum at 1.7% of the central intensity for the disc, 4.5% for the square),
- secondary minima are periodically distributed for the square, not for the disc.

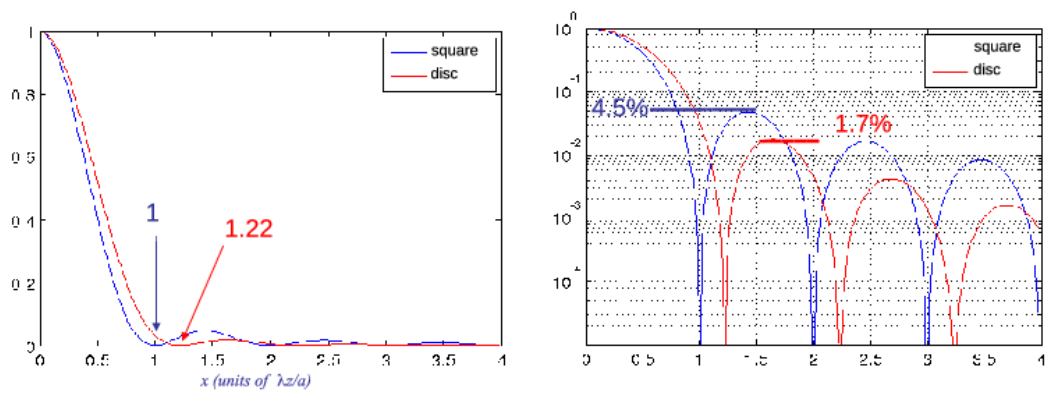


Figure 1.9: Comparison between Fraunhofer diffraction patterns of a disc of diameter a and a square aperture of same side a . Left: graph of the intensities (normalised so that the maximum is 1). Right: same in semi-logarithmic scale.

Chapter 2

Fourier properties of converging lenses

Also read:

- Goodman, J.W., “Introduction to Fourier Optics”, chap 5

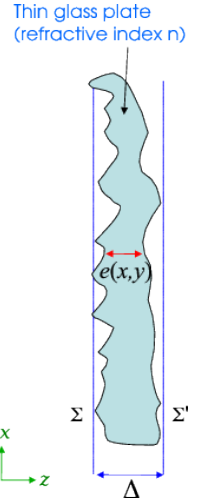
2.1 Phase screens

2.1.1 Transmission coefficient of a thin phase screen

It can be considered that transparent objects with variable thickness $e(x, y)$ (e.g. prisms, lenses, glass plates) and/or variable refraction index $n(x, y)$ (for example a layer of gas with inhomogeneous temperature) act as screens introducing a phase shift. The associated transmission coefficient $t(x, y)$ is a complex phase term which takes the form :

$$t(x, y) = e^{ik\Delta} \exp [ik(n - 1)e(x, y)] \quad (2.1)$$

with k the wave number of the incoming light and Δ the maximal thickness of the plate. Paraxial approximation is assumed here so that we consider that the trajectory in the material is $e(x, y)$ whatever the incidence of the wave, neglecting effects of inclinations. This relation is true only if the phase screens are thin.



Proof: The plate is enclosed between two parallel planes (see graph above) Σ (corresponding to $z = 0$) and Σ' (at $z = \Delta$). We consider a plane incident wave with normal incidence. Its complex amplitude at the entrance plane Σ is a constant

$$f_0(x, y) = A$$

In the exit plane $z = \Delta$, the light ray crossing the point (x, y) has travelled a distance $e(x, y)$ in the material¹, and $\Delta - e(x, y)$ in the vacuum, so that the complex amplitude is

$$f_\Delta(x, y) = A e^{ik n e(x, y)} e^{ik(\Delta - e(x, y))}$$

which is the product of two terms:

$$f_\Delta(x, y) = f_0(x, y) e^{ik\Delta} \exp[ik(n - 1)e(x, y)] \quad (2.2)$$

the influence of the plate is a multiplicative term $t(x, y) = e^{ik\Delta} \exp[ik(n - 1)e(x, y)]$.

We generally neglect the constant term $e^{ik\Delta}$ and write the transmission coefficient of the plate as

$$\boxed{t(x, y) = \exp [ik(n - 1)e(x, y)]} \quad (2.3)$$

¹assuming that the ray goes almost parallel to the z axis so that it hits the planes Σ and Σ' at the same transverse coordinates (x, y) : this approximation is possible only for thin plates.

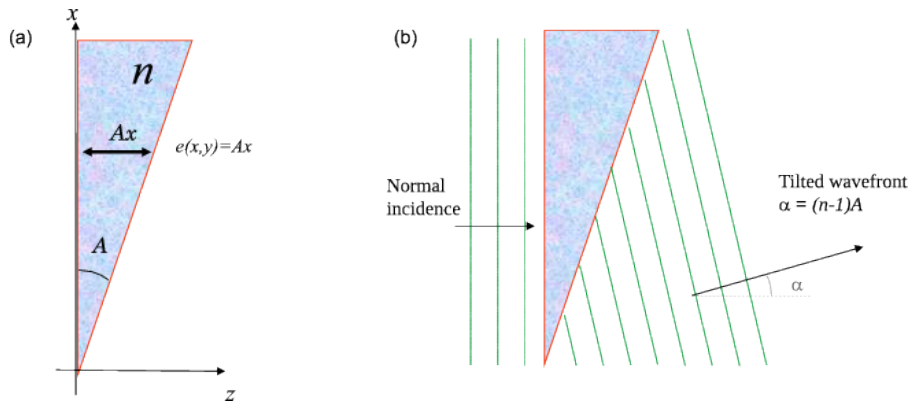


Figure 2.1: (a): glass prism of refraction index n . The thickness function is $e(x, y) = Ax$ with $A \ll 1$. (b): illustration of the deviation of a plane wave with normal incidence by the prism. The new incidence is $\alpha = (n - 1)A$.

2.1.2 Example: prism

We consider the glass prism of Fig. 2.1a with a thickness $e(x, y) = Ax$ and $A \ll 1$. The transmission of this prism is

$$t(x, y) = \exp[ik(n - 1)Ax] \quad (2.4)$$

Note that we have neglected the edges of the prism, considering that it has an infinite extension in the plane (x, y) . The above transmission coefficient is indeed to be multiplied by an adequate rectangular function. If the prism is lit by a plane wave under normal incidence and complex amplitude ψ_0 at the entrance plane of the prism (taken as $z = 0$), then the exit amplitude (in the plane $z = 0$)² is

$$f(x, y) = \psi_0 e^{ik(n-1)Ax} \quad (2.5)$$

which is, in paraxial approximation, the amplitude of a plane wave (linear phase in x , see Section 1.1.2) of wave vector

$$\vec{k} = \frac{2\pi}{\lambda} \begin{cases} \alpha = (n - 1)A \\ \beta = 0 \\ \gamma \end{cases} \quad \text{the coefficient } \gamma \text{ does not appear explicitly here since the amplitude is written in the plane } z = 0.$$

It can be calculated using the relation $\alpha^2 + \beta^2 + \gamma^2 = 1$. Note that the tilt angle of this wave is $(n - 1)A$, a result well-known in geometric optics (see Fig. 2.1b).

2.1.3 Converging lens

We consider a plano-convex lens of refraction index n and radius of curvature R (Fig. 2.2a). The curved surface is a portion of sphere which can be approximated by a paraboloid if the lens is thin (e.g. $R \gg \Delta$). In this case the thickness function expresses as

$$e(x, y) \simeq \Delta - \frac{\rho^2}{2R} \quad (2.6)$$

with $\rho^2 = x^2 + y^2$. The transmission coefficient (neglecting the constant term in Δ) is

$$t(x, y) = \exp \left[-ik(n - 1) \frac{\rho^2}{2R} \right] \quad (2.7)$$

let's introduce the *focal length* F of the lens

$$F = \frac{R}{n - 1} \quad (2.8)$$

the transmission of the lens is a quadratic phase term which will now be denoted using the notation $L_F(x, y)$:

$$L_F(x, y) = \exp \left[-\frac{i\pi\rho^2}{\lambda F} \right]$$

(2.9)

As for the example of the prism above, we have neglected the edges of the lens, considering an infinite extension in the (x, y) plane. The complete transmission coefficient is obtained by multiplying $L_F(x, y)$ by a 2D circular function.

²the exit amplitude should be written in the exit plane $z = \Delta$ with Δ the maximum thickness of the prism. However we neglected the term $e^{ik\Delta}$ in the transmission coefficient: that is similar to write the exit amplitude back in the plane $z = 0$.

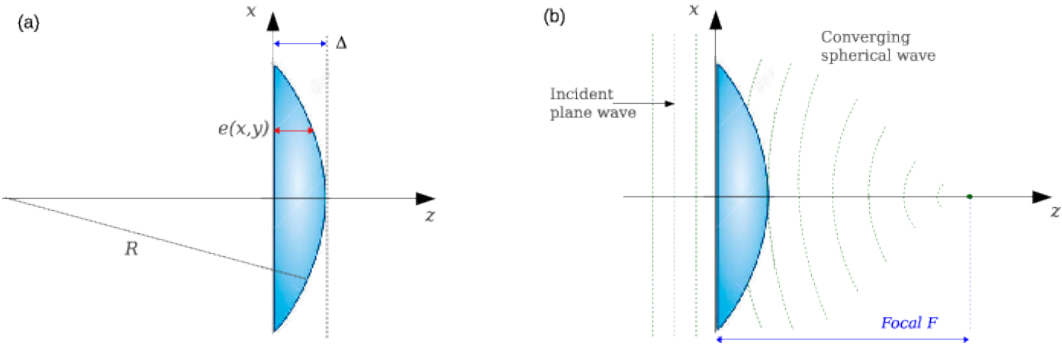


Figure 2.2: (a): Plano-convex lens of refraction index n . The exit surface is a portion of sphere of radius of curvature R and maximum thickness Δ . (b): Transformation of an incident plane wave into a converging spherical wave at the exit of the lens. The center of this converging wave is at $z = F$ (focal length of the lens).

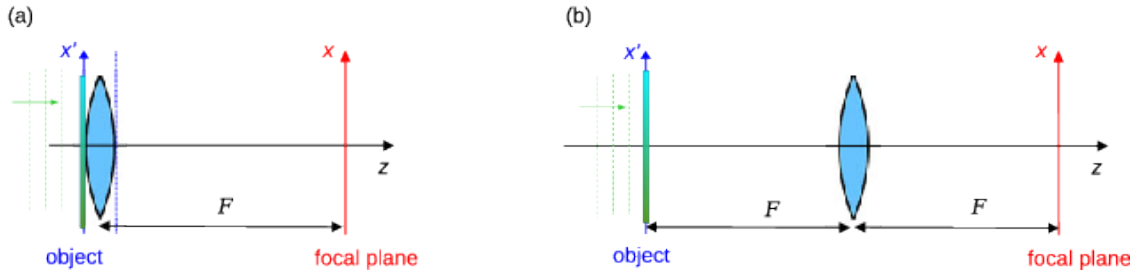


Figure 2.3: Optical scheme for the observation of the 2D Fourier transform of the transmission of an object using a converging lens. (a): Object in the same plane as the lens. (b): Object at the front focal plane of the lens.

If the lens is lit by a plane wave under normal incidence and complex amplitude ψ_0 at the entrance plane of the lens (plane $z = 0$), then the exit amplitude (in the plane $z = 0^+$) is

$$f_{0+}(x, y) = \psi_0 e^{-\frac{i\pi\rho^2}{\lambda F}} \quad (2.10)$$

the quadratic phase term in x and y is the signature of a spherical wave under paraxial approximation (see Section 1.1.3) of center $(0, 0, F)$, and the minus sign in the exponential shows that this is a converging wave. This is illustrated by the figure 2.2b. The plane $z = F$ is called *back focal plane* (or just “focal plane”) of the lens.

Case of a diverging lens: a simular calculation shows that the transmission of a diverging lens of focal F is obtained by changing F into $-F$ in the equation 2.9, so that it can be denoted as “ $L_{-F}(x, y)$ ”:

$$L_{-F}(x, y) = \exp \left[+\frac{i\pi\rho^2}{\lambda F} \right] \quad (2.11)$$

It is thus possible to define a *generalized focal length*, positive for a converging lens and negative for a diverging lens, and use Eq. 2.9 for both cases.

2.2 Converging lenses and Fourier transform

In this section we consider an ensemble formed by an object of transmission $t(x, y)$ and a converging lens. This ensemble is lit under normal incidence by a plane wave. The aim is to write down the complex amplitude at the focal plane of the lens. Two cases will be considered:

- the object is attached to the lens (they are in the same plane),
- the object is in the *front focal plane* of the lens (distance $z = -F$ from the lens)

The figure 2.3 shows the optical configuration for the two cases.

2.2.1 Object in the same plane as the lens

We use the following conventions:

- the plane of the object/lens is at $z = 0$
- coordinates in the plane $z = 0$ are denoted (x', y') , and (x, y) in the focal plane $z = F$
- the complex amplitude of the incident wave (for $z < 0$) is $\psi_0 e^{ikz}$ (normal incidence, $\vec{k} \parallel \hat{z}$)

The optical configuration is shown in Fig. 2.3a. To calculate the complex amplitude in the plane $z = F$, we have to write the amplitude just after the lens ($z = 0^+$), then do a Fresnel diffraction to the plane $z = F$.

The complex amplitude just before the lens ($z = 0^-$) is the product

$$f_0(x', y') = \psi_0 t(x', y') \quad (2.12)$$

After the lens, it becomes

$$f_{0+}(x', y') = f_0(x', y') L_F(x', y') \quad (2.13)$$

The Fresnel diffraction to the plane $z = F$ is given by Eq 1.17:

$$f_F(x, y) = e^{ikF} f_{0+}(x, y) * D_F(x, y) \quad (2.14)$$

with $D_F(x, y) = \frac{1}{i\lambda F} e^{\frac{i\pi\rho^2}{\lambda F}}$. By expanding the convolution product, it can be put into the following form (known as *Fresnel transform*):

$$f_F(x, y) = \frac{e^{ikF}}{i\lambda F} e^{\frac{i\pi\rho^2}{\lambda F}} \mathcal{F} \left[f_{0+}(x', y') e^{\frac{i\pi\rho'^2}{\lambda F}} \right]_{u=\frac{x}{\lambda F}, v=\frac{y}{\lambda F}} \quad (2.15)$$

with $\rho'^2 = x'^2 + y'^2$ and \mathcal{F} the Fourier transform. The curvature phase term $e^{\frac{i\pi\rho'^2}{\lambda F}}$ in the brackets simplifies with the coefficient $L_F(x', y')$ so that the complex amplitude in the focal plane is

$$f_F(x, y) = \frac{e^{ikF}}{i\lambda F} e^{\frac{i\pi\rho^2}{\lambda F}} \hat{f}_0 \left(\frac{x}{\lambda F}, \frac{y}{\lambda F} \right) \quad (2.16)$$

Hence, in the focal plane the amplitude is proportional to the Fourier transform of the amplitude in the plane $z = 0$. The intensity is

$$I(x, y) = \frac{1}{\lambda^2 F^2} \left| \hat{f}_0 \left(\frac{x}{\lambda F}, \frac{y}{\lambda F} \right) \right|^2 \quad (2.17)$$

As for a Fraunhofer diffraction (see Section 1.2.3), it is possible to observe the 2D power spectrum $|\hat{f}_0(u, v)|^2$ of the complex amplitude at the entrance of the lens. Note that this observation is valid only in the focal plane of the lens (otherwise a Fresnel diffraction between the focal plane and the observation plane applies).

An astrophysical application of this Fourier property was made by Labeyrie in 1970 in his historical paper about speckle interferometry (Labeyrie A., 1970, “Attainment of Diffraction Limited Resolution in Large Telescopes by Fourier Analysing Speckle Patterns in Star Images”, A&A **6**, 85). Labeyrie needed to accumulate power spectra of short exposure photographs of stars, and he did it using an optical bench (a laser beam passing through the photographic film, a lens and a photographic plate recording the power spectrum).

In the absence of object ($t(x', y') = 1$) the diffracted amplitude is proportional to a Dirac function $\delta(x, y)$, which explicits the focusing effect of a converging lens on the axis.

The multiplicative phase curvature $e^{\frac{i\pi\rho^2}{\lambda F}}$ in Eq. 2.16 may be cancelled by adding a second converging lens of focal F in the focal plane. But we shall see hereafter that this phase term vanishes if the object is placed at the distance F in front of the lens.

2.2.2 Object at the front focal plane

The optical scheme is shown in Fig. 2.3b. The object is at a distance F in front of the lens (front focal plane). To calculate the amplitude at the back focal plane $z = 2F$ we use a plane by plane approach, and successively calculate complex amplitudes in the 3 planes of interest (object, lens, focal).

Object plane $z = 0$: the complex amplitude just after the object is denoted as $f_0(x', y')$ as in the paragraph before.

Lens plane, just before the lens ($z = F^-$): we apply a Fresnel diffraction (Eq 1.17) between the planes $z = 0$ and $z = F$:

$$f_F(x, y) = e^{ikF} f_0(x, y) * D_F(x, y) \quad (2.18)$$

Focal plane, $z = 2F$: we can apply the result of the paragraph above (Eq. 2.16), the amplitude $f_F(x, y)$ plays here the same role as f_0 in Eq. 2.16:

$$f_{2F}(x, y) = \frac{e^{ikF}}{i\lambda F} e^{\frac{i\pi\rho^2}{\lambda F}} \hat{f}_F\left(\frac{x}{\lambda F}, \frac{y}{\lambda F}\right) \quad (2.19)$$

using the expression of $f_F(x, y)$ we have

$$f_{2F}(x, y) = \frac{e^{ikF}}{i\lambda F} e^{\frac{i\pi\rho^2}{\lambda F}} \mathcal{F}[e^{ikF} f_0(x, y) * D_F(x, y)]_{u=\frac{x}{\lambda F}, v=\frac{y}{\lambda F}} \quad (2.20)$$

which gives

$$f_{2F}(x, y) = \frac{e^{2ikF}}{i\lambda F} e^{\frac{i\pi\rho^2}{\lambda F}} \hat{f}_0\left(\frac{x}{\lambda F}, \frac{y}{\lambda F}\right) \cdot \hat{D}_F\left(\frac{x}{\lambda F}, \frac{y}{\lambda F}\right) \quad (2.21)$$

The Fourier transform of D_F is $\hat{D}_F(u, v) = \exp[-i\pi\lambda F(u^2 + v^2)]$. It simplifies with the curvature phase term $e^{\frac{i\pi\rho^2}{\lambda F}}$, and we finally obtain

$$\boxed{f_{2F}(x, y) = \frac{e^{2ikF}}{i\lambda F} \hat{f}_0\left(\frac{x}{\lambda F}, \frac{y}{\lambda F}\right)} \quad (2.22)$$

The phase curvature $e^{\frac{i\pi\rho^2}{\lambda F}}$ has now been cancelled and we obtain the exact Fourier transform of the amplitude f_0 of the object, scaled by a factor $\frac{1}{\lambda F}$ in both directions x and y . The relation between f_0 and f_{2F} will be denoted as “optical Fourier transform”.

It can be shown that these results remain valid whatever the position of the object before the lens, providing that the lens is large enough to collect all the light diffracted by the object. Moving the object along the z axis changes only the phase curvature term in Eq. 2.16 but the intensity remains the same.

In the case where the object is placed after the lens, in the converging light beam, one still observes its 2D Fourier transform but there is a scale factor depending on the distance between the lens and the object. We then have a “zoom” effect on the power spectrum by varying the distance.

Chapter 3

Coherent optical filtering

Also read:

- Goodman, J.W., “Introduction to Fourier Optics”, chap 8

3.1 Principle

In electronics, or signal processing, the frequency filtering is the operation which consists to multiply the frequency spectrum of a given temporal signal by a function called “filter”. The result is a convolution of the signal by an impulse response, which is the inverse Fourier transform of the filter. In optics, this operation is made on 2D functions, and is a filtering of *spatial frequencies*.

It is very easy to perform: we showed in section 2.2.2 that a converging lens of focal F forms, in its focal plane, the 2D Fourier transform $\hat{t}\left(\frac{x}{\lambda F}, \frac{y}{\lambda F}\right)$ of an object of transmission $t(x, y)$. It is therefore possible to multiply this Fourier transform by placing objects in the focal plane of the lens. We will denote this focal plane as “filtering plane”, since the filtering is performed in this particular plane. Objects such as slits or diaphragms will act on the modulus of \hat{t} . Transparent objects with a given index of refraction and thickness will act on the phase of \hat{t} .

To observe the result of the filtering in the direct plane, one needs to perform an inverse Fourier transform. In signal processing, this is done by a dedicated software. In optics, one can take advantage of the following remarkable Fourier property:

$$\hat{f}(u, v) \xrightarrow{\mathcal{F}} f(-x, -y) \quad (3.1)$$

hence, a direct Fourier transform is similar to an inverse Fourier transform, with a change of the sign of the variables x and y (resulting in a 180° rotation of the function f). This property allows to observe the result of an optical filtering by placing a second lens after the filtering plane: in the focal plane of this second lens one observes the 2D inverse Fourier transform of the filtered spectrum \hat{t} , i.e. the filtered object, rotated by 180° .

This two-lens system is also known as “double diffraction setup” (see Fig. 3.1), each lens performing an optical Fourier transform (analogous to a Fraunhofer diffraction). Note that the two lenses may have different focal lengths, but the filtering plane has to be at the front focal plane of the second lens (conjugated lenses) in order to avoid unwanted phase curvature terms in the optical Fourier transforms.

3.2 Abbe-Porter experiments

Pioneering experiments were made in the early 1900's and give a spectacular illustration of image formation and Fourier optics fundamentals. They consist in simple filtering of spatial frequencies, as described in the previous section. The principle is the following: a fine 2D metallic grid is lit by a laser beam (Fig. 3.2). This object is placed at the front focal plane of the first lens (plane P_0). In the filtering plane (P_1) one observes the Fourier transform of the object. It is composed of bright spots (since the object is periodic), every spot being an Airy disc if the grid is limited by a circular diaphragm. In the focal plane of the second lens (observation plane, P_2), one observes a replica of the object, convoluted by the PSF of the filter (see section 3.3 for details). If no filter is placed in the filtering plane, the image is identical to the object (rotated by 180°).

In the filtering plane, bright spots along the horizontal (resp. vertical) axis correspond to horizontal (resp. vertical) spatial frequencies composing the object. We suppose that the filter is here a slit which selects one row of bright spots. If the slit is vertical (Fig. 3.3a) it selects only the vertical frequencies of the object: the image in the plane P_2 is a grid with horizontal parallel strips. If the slit is horizontal, (Fig. 3.3b) horizontal frequencies are selected and the image is composed of vertical parallel strips.

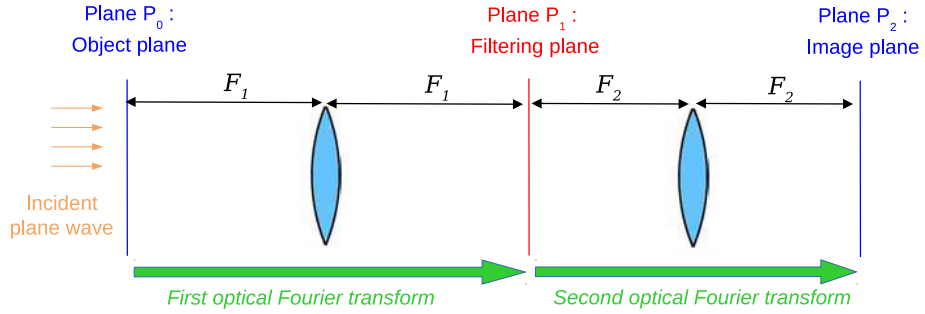


Figure 3.1: Double diffraction setup for optical filtering. The object is placed at the front focal plane of the first lens of focal F_1 and lit by a plane wave. The second lens (focal F_2) is placed at a distance $z = F_1 + F_2$ from the first one, so that the filtering plane is at the front focal plane of the second lens. The observation is made in the back focal plane of the second lens.

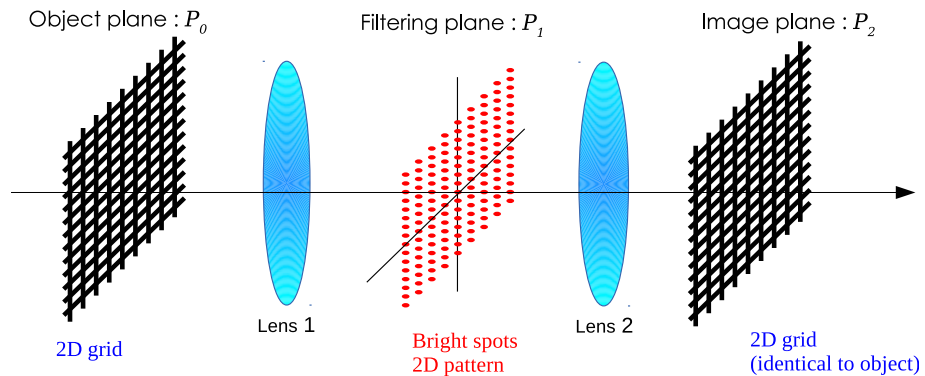


Figure 3.2: Illustration of the Abbe-Porter experiment. A 2D grid is placed in the front object plane P_0 of the first lens. In the focal plane P_1 , one finds the spectrum of the grid, composed of a 2D arrangement of bright spots. If no filter is placed in P_1 , then the second lens forms; at its focal plane P_2 , a replica of the object, rotated by 180° (Fourier transform of its spectrum).

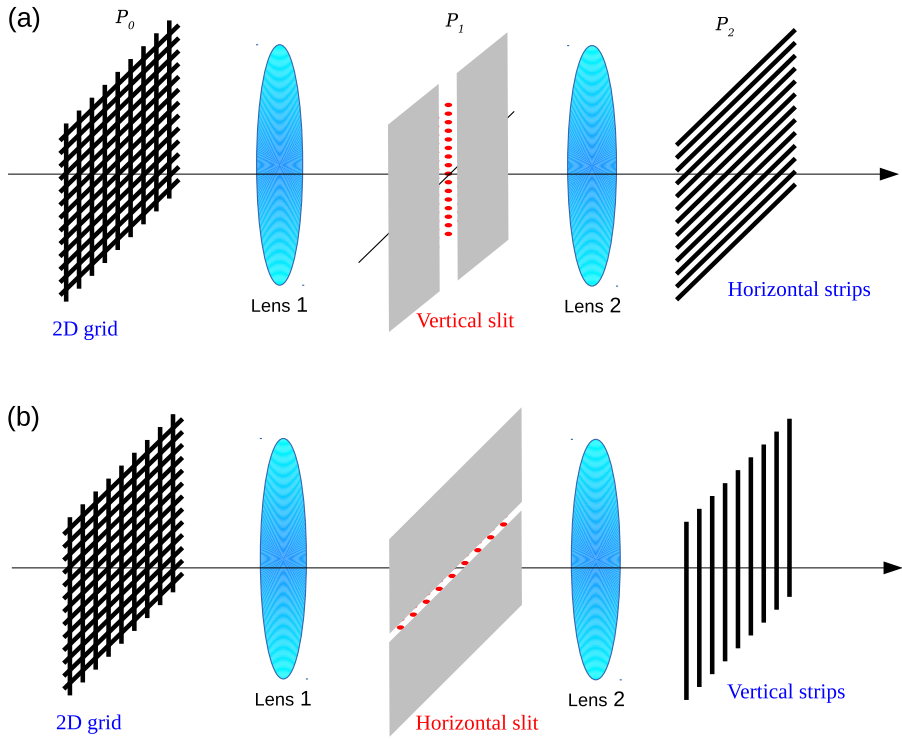


Figure 3.3: Abbe-Porter experiment similar to Fig. 3.2, with a slit in the filtering plane P_1 . (a) vertical slit, selecting the central column of bright spots. The corresponding image in the plane P_2 is a series of horizontal strips, Fourier Transform of the truncated spectrum. (b) horizontal slit, producing in P_2 a set of vertical strips.

3.3 Object-image relation

We consider the double diffraction experiment of Fig. 3.1. The aim of this section is to explicit the relations between the complex amplitudes of the object (plane P_0) and the image in the plane P_2 . We denote as

- ψ_0 the complex amplitude of the incident plane wave in the plane P_0 (normal incidence is assumed)
- F_1 and F_2 the focal length of the two lenses
- (x', y') , (x_1, y_1) and (x, y) the coordinates of a point in the planes P_0 (object plane), P_1 (filtering plane) and P_2 (observation plane)
- $t(x', y')$ the transmission coefficient of the object (plane P_0)
- $P(x_1, y_1)$ the transmission coefficient of the filter (plane P_1)

Let's calculate step by step the propagation from planes P_0 to P_2 : at the output the plane P_0 , the complex amplitude is simply proportional to the transmission of the object:

$$f_0(x', y') = \psi_0 t(x', y') \quad (3.2)$$

We can apply Eq. 2.22 to write the amplitude in the plane P_1 , taking advantage of the Fourier property of the converging lens:

$$f_1(x_1, y_1) = \frac{e^{2ikF_1}}{i\lambda F_1} \hat{f}_0\left(\frac{x_1}{\lambda F_1}, \frac{y_1}{\lambda F_1}\right) \quad (3.3)$$

In the plane P_1 , the filtering operation is performed by multiplying $f_1(x_1, y_1)$ by the transmission of the filter:

$$f_{1+}(x_1, y_1) = \frac{e^{2ikF_1}}{i\lambda F_1} \hat{f}_0\left(\frac{x_1}{\lambda F_1}, \frac{y_1}{\lambda F_1}\right) P(x_1, y_1) \quad (3.4)$$

And to obtain the amplitude in the plane P_2 , we make use, once again, of Eq. 2.22:

$$f_2(x, y) = \frac{e^{2ikF_2}}{i\lambda F_2} \hat{f}_{1+}\left(\frac{x}{\lambda F_2}, \frac{y}{\lambda F_2}\right) \quad (3.5)$$

with

$$\hat{f}_{1+} \left(\frac{x}{\lambda F_2}, \frac{y}{\lambda F_2} \right) = \frac{e^{2ikF_1}}{i\lambda F_1} \mathcal{F} \left[\hat{f}_0 \left(\frac{x_1}{\lambda F_1}, \frac{y_1}{\lambda F_1} \right) P(x_1, y_1) \right]_{u=\frac{x}{\lambda F_2}, v=\frac{y}{\lambda F_2}} \quad (3.6)$$

We eventually obtain a convolution relation:

$$f_2(x, y) = -\frac{1}{G} e^{2ik(F_1+F_2)} f_0 \left(-\frac{x}{G}, -\frac{y}{G} \right) * \frac{1}{(\lambda F_2)^2} \hat{P} \left(\frac{x}{\lambda F_2}, \frac{y}{\lambda F_2} \right) \quad (3.7)$$

where $G = \frac{F_2}{F_1}$ is a magnification factor. The amplitude of the final image in the plane P_2 is thus a convolution between $f_0 \left(-\frac{x}{G}, -\frac{y}{G} \right)$ (the object magnified by a factor G and rotated 180°) and the point-spread function $\frac{1}{(\lambda F_2)^2} \hat{P} \left(\frac{x}{\lambda F_2}, \frac{y}{\lambda F_2} \right)$. The magnification applies before the convolution by the impulse response. The case of identical lenses ($F_1 = F_2$) corresponds to $G = 1$: no magnification, the object and image have the same size.

3.4 Low-pass and high-pass filters

In signal processing, low-pass or high-pass filters attenuate low or high frequencies. The spectrum of the signal is multiplied by a function (denoted as *transfer function*) which vanish for high (resp. low) frequencies in the case of a low-pass (resp. high-pass) filter.

In optics, with a double diffraction experiment, the product between the spectrum of the object and a transfer function appears in Eq. 3.4. For a sake of simplicity, we shall consider the case of two identical lenses ($F_1 = F_2 = F$). Equation 3.4 can be rewritten using the variable change $u = \frac{x_1}{\lambda F}$, $v = \frac{y_1}{\lambda F}$:

$$f_{1+}(\lambda F u, \lambda F v) = \frac{e^{2ikF_1}}{i\lambda F_1} \hat{f}_0(u, v) P(\lambda F u, \lambda F v) \quad (3.8)$$

The right-hand side of this equation lets appear the spectrum $\hat{f}_0(u, v)$ of the object, and the product by the following transfer function:

$$h(u, v) = P(\lambda F u, \lambda F v) \quad (3.9)$$

which is simply a replica of the pupil function, magnified by a factor $\frac{1}{\lambda F}$.

3.4.1 Low-pass filters

A low-pass filter has a transfer function which vanish for high frequencies. A circular diaphragm of diameter d , centered on the optical axis in the filtering plane, is an example of low-pass filter. The corresponding transfer function is

$$h(u, v) = \prod \left(\frac{\lambda F q}{d} \right) \quad \text{with } q^2 = u^2 + v^2 \quad (3.10)$$

This transfer function is isotropic, and vanishes for spatial frequencies $q > f_c$ with $f_c = \frac{d}{2\lambda F}$ the *cutoff frequency*. Let's consider the case where the object is a sinusoidal grid of spatial frequency m whose transmission (between 0 and 1) is

$$t(x, y) = \frac{1}{2} + \frac{1}{2} \cos(2\pi m x) \quad (3.11)$$

its Fourier transform is composed of 3 Dirac peaks centered at frequencies $(0, 0)$, $(m, 0)$ and $(-m, 0)$

$$\hat{t}(u, v) = \frac{1}{2} \delta(u, v) + \frac{1}{4} \delta(u - m, v) + \frac{1}{4} \delta(u + m, v) \quad (3.12)$$

Multiplying this spectrum by the transfer function of Eq. 3.10 will cut the lateral peaks if $m > f_c$. In this case, the image in the plane P_2 will be uniform. This is illustrated by Fig. 3.4. For a more general object $t(x, y)$ having a continuous frequency spectrum $\hat{t}(u, v)$, a low-pass filter will remove high frequencies, resulting into a fuzzy image with a loss of details, as illustrated by Fig. 3.5.

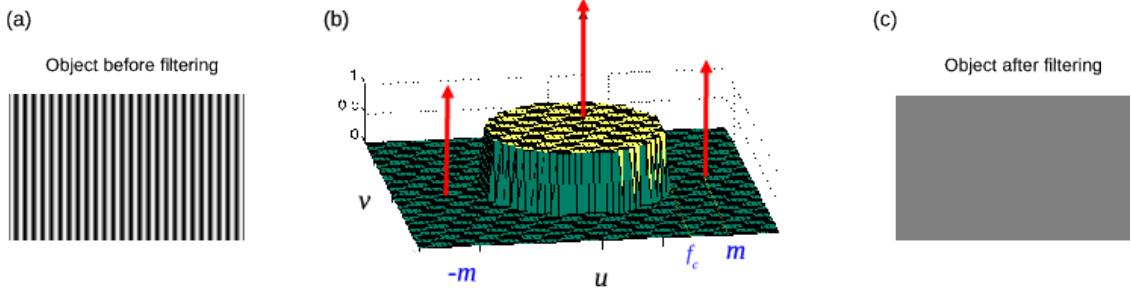


Figure 3.4: Low-pass filtering of a sinusoidal grid of spatial frequency m by a circular transfer function of cutoff frequency $f_c < m$ (see § 3.4.1). (a) grayscale plot of the transmission of the object. (b) Perspective plot showing the transfer function (Eq. 3.10) and the 3 peaks of the Fourier transform of the object (Eq. 3.12). Since $m > f_c$ the two lateral peaks are cut by the transfer function. (c) Resulting image (uniform) in the observation plane P_2 .

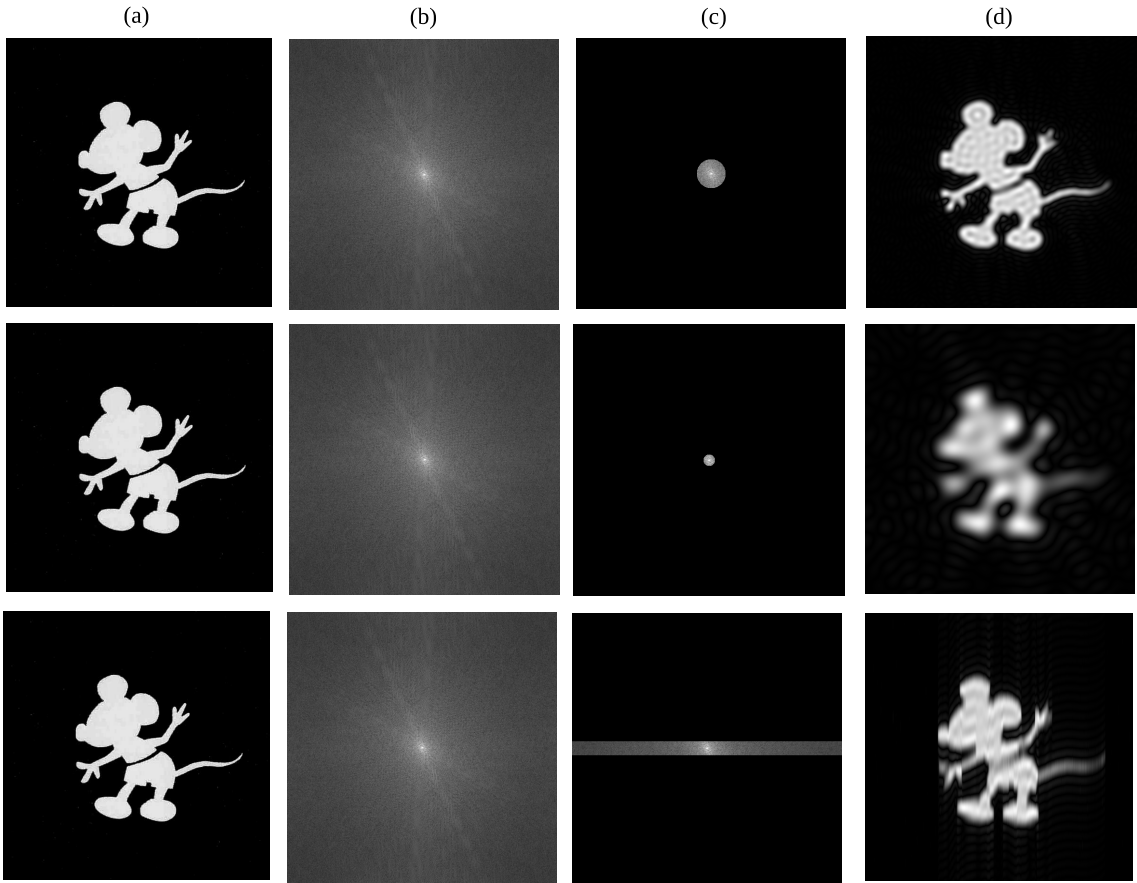


Figure 3.5: Low-pass filtering of an object (Mickey shape) for 3 different filters. (a) Object. (b) Spectrum of the object (modulus). (c) Spectrum of the object (modulus) multiplied by the transfer function of the filter. (d) Resulting image in the observation plane (without the 180° rotation). 1st row: the filter is a circular pupil. 2nd row: the filter is also a circular pupil, but with lower diameter (resulting in a more fuzzy resulting image). 3rd row: the filter is an horizontal slit; it is still a low-pass filter, but in the vertical direction only.

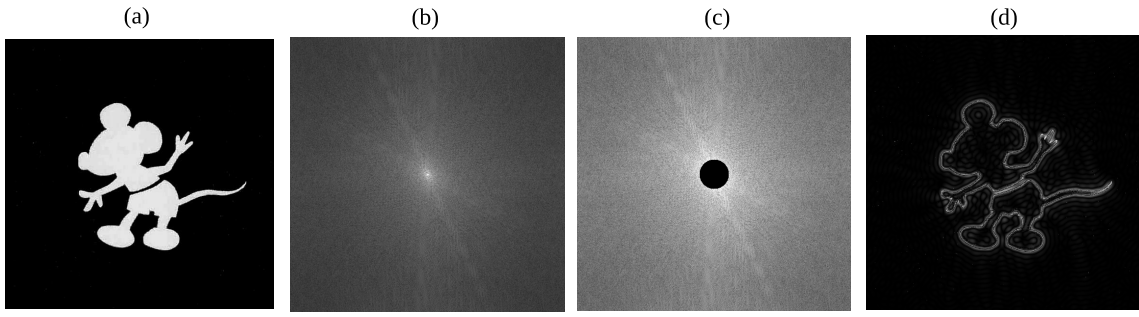


Figure 3.6: High-pass filtering of an object (Mickey shape). (a) Object. (b) Spectrum of the object (modulus). (c) Spectrum of the object (modulus) multiplied by the transfer function of the filter. (d) Resulting image in the observation plane (without the 180° rotation). The filter is here a circular occulter having the same diameter as the circular hole of the 1st row of Fig. 3.5.

3.4.2 High-pass filters

A high-pass filter has a transfer function which vanish for low frequencies. An example is a on-axis circular occulter of placed in the filtering plane P_1 which blocks the light up to a certain distance from the center. This kind of filter tends to reinforce high spatial frequencies in the image and to emphasize fine details – exactly the opposite of the low-pass filter.

Fig. 3.6 shows the effet of a high-pass filtering by a circular diaphragm on a “Mickey” object similar to the figure 3.5. The filtered image displays only the contours of Mickey, everything else has been removed by the filter. This reinforcement of the contours is easy to understand if one remarks that the filter (circular occulter) is the complementary screen of a circular diaphragm. Its transmission expresses as

$$P_o(x, y) = 1 - P(x, y) \quad (3.13)$$

with $P(x, y) = \Pi\left(\frac{\rho}{d}\right)$ the transmission of the circular diaphragm. Therefore the point-spread function of the filtering (appearing in Eq. 3.7) is

$$\hat{P}_o\left(\frac{x}{\lambda F}, \frac{y}{\lambda F}\right) = (\lambda F)^2 \delta(x, y) - \hat{P}\left(\frac{x}{\lambda F}, \frac{y}{\lambda F}\right) \quad (3.14)$$

and the amplitude in the observing plane, given by Eq. 3.7, expresses as the difference of two terms

$$f_2(x, y) = -e^{4ikF} \left[\underbrace{f_0(-x, -y)}_{\text{amplitude of the unfiltered object}} - \underbrace{f_0(-x, -y) * \frac{1}{(\lambda F)^2} \hat{P}\left(\frac{x}{\lambda F}, \frac{y}{\lambda F}\right)}_{\text{low-pass filtered object}} \right] \quad (3.15)$$

The first term is the amplitude of the unfiltered object, i.e. the “Mickey” object (Fig. 3.5, column a). The second term is the amplitude of object filtered by the circular diaphragm, it is a smoothed version of “Mickey” (Fig. 3.5, 1st row, column d). The first term has sharpest countours than the second, this is why their difference let only appear only the countours of the object.

Other spectacular illustrations of optical filtering of 2D objects can be found in the book “Atlas of Optical Transforms” by Harburn.

3.5 Strioscopy and phase contrast

Optical filtering techniques can be applied to phase objects, i.e. transparent objects with variable thickness or refraction index (for example a fingerprint on a microscope plate). Phase variations of the object can be made visible by placing an appropriate mask in the filtering plane of a double-diffraction setup.

For the whole paragraph, we consider the optical setup of Fig. 3.1, with identical lenses ($F_1 = F_2 = F$). The object in the plane P_0 is a pure phase object of transmission

$$t(x, y) = e^{i\phi(x, y)} \quad (3.16)$$

lit by an incident plane wave of amplitude ψ_0 . With the condition $\phi(x, y) \ll 1$ (small phase variations), the transmission can be approximated to the first-order development

$$t(x, y) \simeq 1 + i\phi(x, y) \quad (3.17)$$

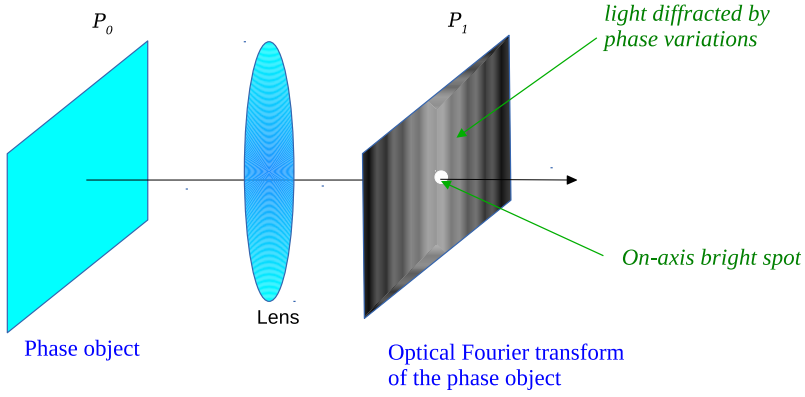


Figure 3.7: Optical Fourier transform of a phase object with small phase variations. The complex amplitude in the focal plane of the lens (P_1) shows a bright central spot surrounded by a halo of light diffracted by phase variations of the object (see Eq. 3.18).

The complex amplitude in the plane P_1 , given by Eq. 3.3, is composed of two terms:

$$f_1(x_1, y_1) = \psi_0 \frac{e^{2ikF}}{\lambda F} \left[\underbrace{-i(\lambda F)^2 \delta(x_1, y_1)}_{\text{bright central spot}} + \underbrace{\hat{\phi}\left(\frac{x_1}{\lambda F}, \frac{y_1}{\lambda F}\right)}_{\text{light diffracted by phase variations}} \right] \quad (3.18)$$

There is a bright spot at the origin, surrounded by a halo of light diffracted by the phase variations $\phi(x, y)$ of the object. This halo of light is faint because $\phi(x, y) \ll 1$, and disappears if $\phi = 0$, i.e. is there is no object in the plane P_0 (in this case the bright central spot is simply the light of the incident plane wave, focused by the lens L_1). This is illustrated by Fig. 3.7. If no filter is placed in the plane P_1 , one observes, in the image plane P_2 , a complex amplitude

$$f_2(x, y) = e^{4ikF} \psi_0 t(-x, -y) \quad (3.19)$$

and the intensity is uniform since $|t(-x, -y)|^2 = 1$. This means that the phase variations of the object are invisible on the image. To make them visible, several kinds of filters can be placed in the plane P_1 . We shall study two of them in the following: an amplitude filter (strioscopy technique) and a phase filter (phase-contrast technique).

3.5.1 Strioscopy

In the technique of strioscopy, the filter is a circular occulter of very small diameter (like a pinhead), centered on the optical axis. It is a high-pass filter which blocks only the spatial frequency $(0, 0)$. The optical setup is shown in Fig. 3.8.

The action of the occulter is to cancel the Dirac peak appearing in the complex amplitude in the plane P_1 (Eq. 3.18). At the output of the filter, the complex amplitude becomes

$$f_{1+}(x_1, y_1) \simeq \psi_0 \frac{e^{2ikF}}{\lambda F} \hat{\phi}\left(\frac{x_1}{\lambda F}, \frac{y_1}{\lambda F}\right) \quad (3.20)$$

Note that the occulter cancels also a part of the term $\hat{\phi}\left(\frac{x_1}{\lambda F}, \frac{y_1}{\lambda F}\right)$ near the origin, but since we made the hypothesis that the occulter is very small, this effect will be neglected. The complex amplitude in the observation plane P_2 is

$$f_2(x, y) = -i e^{4ikF} \psi_0 \phi(-x, -y) \quad (3.21)$$

and the intensity is

$$I_2(x, y) = |\psi_0|^2 |\phi(-x, -y)|^2 \quad (3.22)$$

it is proportional to the square of the phase variations of the object. Therefore the object phase is made visible by this strioscopy technique. Similar results can be obtained by replacing the occulter in the plane P_1 by a half plane (Foucault knife-edge technique). Spectacular videos can be found on the web, see for example

<https://www.futura-sciences.com/sciences/videos/voir-invisible-strioscopie-822/>.

However this technique has the disadvantage that the sign of the phase is lost (i.e. it is impossible to know if a given structure in the image corresponds to a bump or a hole on the object). Also, since the phase variations $\phi(x, y)$ are small, images are very faint. The alternative technique of “phase contrast”, presented hereafter, provides an answer to these problems.

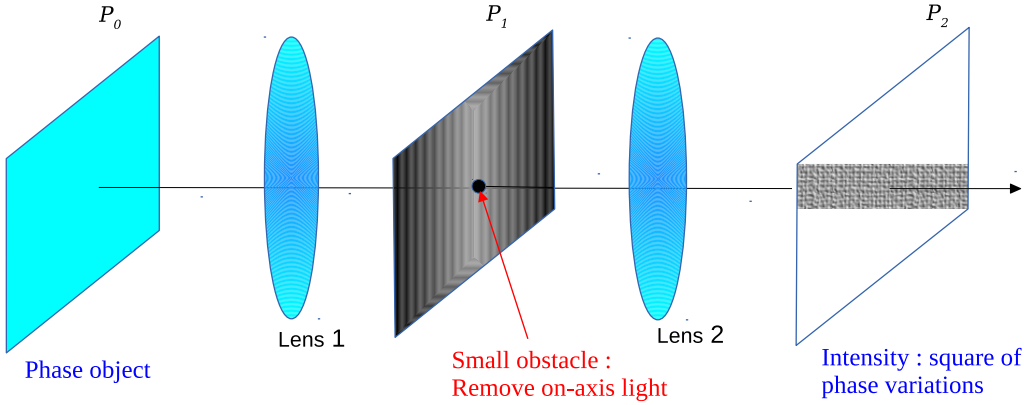


Figure 3.8: Strioscopy technique applied to a phase object placed in the plane P_0 . In the Fourier plane (P_1), there is a central bright spot (see Eq. 3.18) which is cancelled by a small occulter. In the image plane P_2 , the intensity is proportional to the square of the phase variations of the object.

3.5.2 Phase contrast

The technique of phase contrast was proposed by Zernike in the early 30s (Zernike F., 1934, MNRAS 94, 377). It appeared to have many applications in microscopy to study quasi-transparent living cells. Zernike was awarded the Nobel prize in 1953 for the phase-contrast micropscopy technique. Phase contrast is similar to strioscopy: the difference is that the occulter is no more opaque, but is a small parallel plate producing a $\frac{\pi}{2}$ phase shift to the on-axis light. The complex amplitude in the plane P_1 at the output of the plate becomes

$$f_{1+}(x_1, y_1) = \psi_0 \frac{e^{2ikF}}{\lambda F} \left[(\lambda F)^2 \delta(x_1, y_1) + \hat{\phi} \left(\frac{x_1}{\lambda F}, \frac{y_1}{\lambda F} \right) \right] \quad (3.23)$$

and in the observation plane

$$f_2(x, y) = -i e^{4ikF} \psi_0 [1 + \phi(-x, -y)] \quad (3.24)$$

The corresponding intensity is (under the hypothesis $\phi(x, y) \ll 1$)

$$I_2(x, y) \simeq |\psi_0|^2 [1 + 2\phi(-x, -y)] \quad (3.25)$$

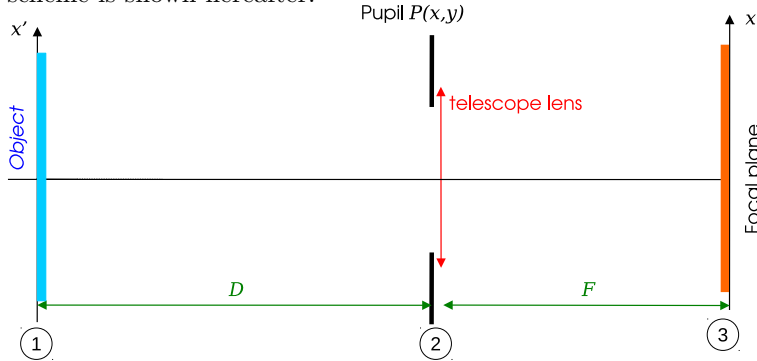
it is now an affine function of the phase $\phi(x, y)$, composed of a constant term (uniform light background) and intensity variations proportionnal to the phase of the object, with its sign: brightest (resp. darkest) zones in the image correspond to positive (resp. negative) phase value.

Chapter 4

Image formation

Also read : Goodman J.W., ‘Introduction to Fourier Optics’, chap. 6

The aim of this chapter is to derive the object-image relation between intensities of an astronomical object and its image at the focus of a telescope. The object is supposed to be incoherent and at large distance from the telescope. The optical scheme is shown hereafter:



We use the following conventions:

Plane ①: Astronomical object (distance from the telescope is D , can be several parsecs)

Plane ②: Converging lens (focal F) + pupil function $P(x, y)$ (in most cases a uniform disc)

Plane ③: Image plane = focal plane of the telescope.

Principle of the calculation:

- Place a point-source at position (x_0, y_0) in plane ①.
- Calculate the corresponding intensity in plane ③, using Fourier properties of lenses
- Sum on (x_0, y_0) to obtain the intensity produced by any object in plane ①.

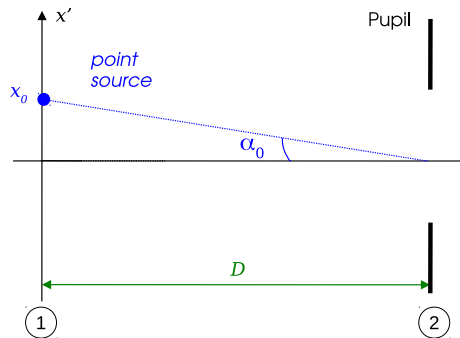
4.1 Object-image convolution relation

4.1.1 Image created by a point-source

In plane ①

Coordinates the plane ① are denoted as (x', y') . A point-source is placed at position (x_0, y_0) : its complex amplitude is $f_1(x', y') = a_0\delta(x' - x_0, y' - y_0)$ where a_0 is a constant. We change to the following angular variables

$$\begin{bmatrix} \alpha' = \frac{x'}{D} \\ \beta' = \frac{y'}{D} \end{bmatrix} \quad \begin{bmatrix} \alpha_0 = \frac{x_0}{D} \\ \beta_0 = \frac{y_0}{D} \end{bmatrix} \quad (4.1)$$



so that the complex amplitude writes as

$$f_1(x', y') = a_0 \delta(x' - x_0, y' - y_0) = \frac{a_0}{D^2} \delta(\alpha' - \alpha_0, \beta' - \beta_0) = f_0 \delta(\alpha' - \alpha_0, \beta' - \beta_0). \quad (4.2)$$

The corresponding intensity is:

$$I_0 \delta(\alpha' - \alpha_0, \beta' - \beta_0) \quad (4.3)$$

with $I_0 = |f_0|^2$

In plane ②

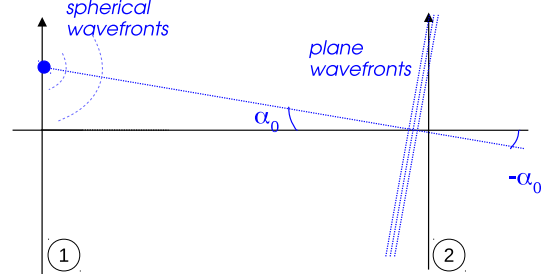
Since D is very large (astronomical distance), Fraunhofer diffraction is assumed between planes ① and ②. Therefore the complex amplitude in plane ②, just before the telescope pupil, is

$$f_2(x, y) = \frac{e^{ikD}}{i\lambda D} \hat{f}_1 \left(\frac{x}{\lambda D}, \frac{y}{\lambda D} \right) \quad (4.4)$$

with $f_1(x', y') = a_0 \delta(x' - x_0, y' - y_0)$ the complex amplitude of the point-source as a function of linear coordinates x' and y' (not angular, to apply the formula for Fraunhofer diffraction). The calculation gives

$$\begin{aligned} f_2(x, y) &= \frac{e^{ikD}}{i\lambda D} a_0 e^{-\frac{2i\pi}{\lambda D}(xx_0+yy_0)} \\ &\downarrow \text{change variable } \alpha_0 = x_0/D, \beta_0 = y_0/D \\ &= \frac{e^{ikD}}{i\lambda D} a_0 e^{-\frac{2i\pi}{\lambda}(\alpha_0 x + \beta_0 y)} \\ &= e^{ikD} \frac{Df_0}{i\lambda} e^{-\frac{2i\pi}{\lambda}(\alpha_0 x + \beta_0 y)} \end{aligned} \quad (4.5)$$

We recognise the complex amplitude of a plane wave with angles of incidence $(-\alpha_0, -\beta_0)$. This is expected, since a point-source emits a spherical wave which becomes plane at large distance.



The complex amplitude just after the pupil is

$$f_{2+}(x, y) = e^{ikD} \frac{Df_0}{i\lambda} e^{-\frac{2i\pi}{\lambda}(\alpha_0 x + \beta_0 y)} P(x, y) \quad (4.6)$$

In plane ③

The complex amplitude just before the telescope lens is $f_{2+}(x, y)$. Therefore the complex amplitude at the focal plane is (see Section 2.2.2, Eq. 2.16):

$$f_3(x, y) = \frac{e^{ikF}}{i\lambda F} \exp \left(\frac{i\pi\rho^2}{\lambda F} \right) \hat{f}_{2+} \left(\frac{x}{\lambda F}, \frac{y}{\lambda F} \right) \quad (4.7)$$

with $\rho^2 = x^2 + y^2$. We get:

$$f_3(x, y) = -\frac{e^{ik(F+D)}}{\lambda^2} \frac{Df_0}{F} \exp \left(\frac{i\pi\rho^2}{\lambda F} \right) \mathcal{F} \left[e^{-\frac{2i\pi}{\lambda}(\alpha_0 x + \beta_0 y)} P(x, y) \right] \quad (4.8)$$

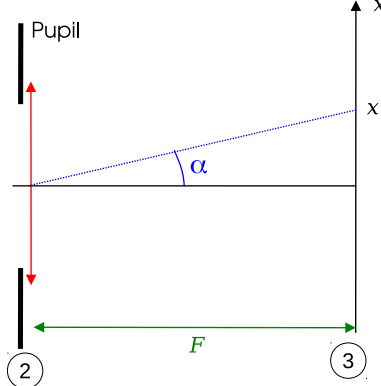
where the Fourier Transform above (\mathcal{F}) is to be taken for variables $u = \frac{x}{\lambda F}$ and $v = \frac{y}{\lambda F}$. Here we have

$$\mathcal{F} \left[e^{-\frac{2i\pi}{\lambda}(\alpha_0 x + \beta_0 y)} P(x, y) \right] = \hat{P} \left(u + \frac{\alpha_0}{\lambda}, v + \frac{\beta_0}{\lambda} \right) \quad (4.9)$$

so

$$\begin{aligned}
 f_3(x, y) &= -\frac{e^{ik(F+D)}}{\lambda^2} \frac{Df_0}{F} \exp\left(\frac{i\pi\rho^2}{\lambda F}\right) \hat{P}\left(\frac{x}{\lambda F} + \frac{\alpha_0}{\lambda}, \frac{y}{\lambda F} + \frac{\beta_0}{\lambda}\right) \\
 &\downarrow \text{change variable } \alpha = x/F, \beta = y/F \\
 &= -\frac{e^{ik(F+D)}}{\lambda^2} \frac{Df_0}{F} \exp\left(\frac{i\pi\rho^2}{\lambda F}\right) \hat{P}\left(\frac{\alpha + \alpha_0}{\lambda}, \frac{\beta + \beta_0}{\lambda}\right)
 \end{aligned} \tag{4.10}$$

The variables α and β represent angles in the image plane as seen from the center of the pupil.



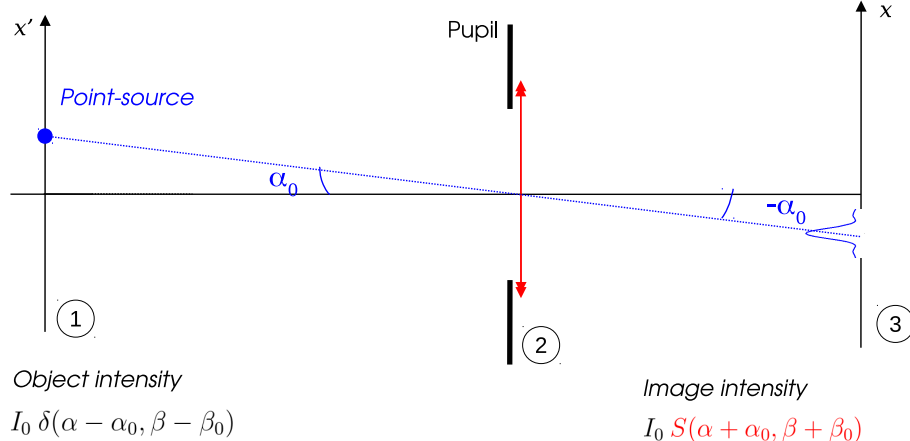
The intensity is $|f_3|^2$. Using angular variables (α, β) , it expresses as

$$|f_3(\alpha, \beta)|^2 = K I_0 \left| \hat{P}\left(\frac{\alpha + \alpha_0}{\lambda}, \frac{\beta + \beta_0}{\lambda}\right) \right|^2 \tag{4.11}$$

where $K = \frac{D^2}{\lambda^4 F^2}$ is a multiplicative constant, generally neglected. We introduce

$$S(\alpha, \beta) = \left| \hat{P}\left(\frac{\alpha}{\lambda}, \frac{\beta}{\lambda}\right) \right|^2 \tag{4.12}$$

so that the intensity is simply $I_0 S(\alpha + \alpha_0, \beta + \beta_0)$ (neglecting the constant K). As a conclusion, we can see that a point-source at position (angle) (α_0, β_0) in plane ① produces an image whose intensity is the Fourier Transform (square modulus) of the pupil function, centered at position $(-\alpha_0, -\beta_0)$. This is illustrated by the following scheme:



Point-Spread Function: The quantity $S(\alpha, \beta)$ is called the *Point-Spread Function* (PSF). It is indeed the image of a point-source of unit intensity ($I_0 = 1$) located on the optical axis ($\alpha_0 = \beta_0 = 0$). It expresses as the power spectrum (square modulus of the Fourier Transform) of the pupil function, as defined in Eq. 4.12

4.1.2 Object-image relation

In plane ① we now consider an *incoherent* object with intensity distribution $I_0(\alpha', \beta')$ as a function of position angles defined by Eq. 4.1. The intensity I_0 can be written as

$$I_0(\alpha', \beta') = I_0 * \delta(\alpha', \beta') = \iint_{-\infty}^{\infty} \underbrace{I_0(\alpha_0, \beta_0)}_{\text{weighting factor}} \underbrace{\delta(\alpha' - \alpha_0, \beta' - \beta_0)}_{\text{unit point-source}} d\alpha_0 d\beta_0 \tag{4.13}$$

This integral can be interpreted as a continuous sum of point-sources located at positions (α_0, β_0) and weighted by the factor $I_0(\alpha_0, \beta_0)$. Each of these point-sources produces in the place ③ a PSF $S(\alpha + \alpha_0, \beta + \beta_0)$, weighted by the same factor, as demonstrated in previous section. Thus the total intensity observed at plane ③ is the continuous sum of intensities¹ produced by each point-source, i.e.

$$\begin{aligned} I(\alpha, \beta) &= \iint_{-\infty}^{\infty} I_0(\alpha_0, \beta_0) S(\alpha + \alpha_0, \beta + \beta_0) d\alpha_0 d\beta_0 \\ &\quad \downarrow \text{change variable } \alpha' = -\alpha_0, \beta' = -\beta_0 \\ &= \iint_{-\infty}^{\infty} I_0(-\alpha', -\beta') S(\alpha - \alpha', \beta - \beta') d\alpha' d\beta' \end{aligned} \tag{4.14}$$

And we obtain the well-known *object-image convolution relation* between intensities, expressed with angular variables:

$$I(\alpha, \beta) = I_0(-\alpha, -\beta) * S(\alpha, \beta) \tag{4.15}$$

The function $I_0(-\alpha, -\beta)$ represents the object rotated by 180° . This relation is valid only for incoherent sources (a similar relation exists between amplitudes for coherent light, see for example the chapter 5 of Goodman, Introduction to Fourier Optics).

Geometric limit, infinite pupil: this is the case where $P(x, y) = 1$. The lens in plane ② has no spatial limitation. The PSF is then a Dirac impulse:

$$S(\alpha, \beta) = \delta(\alpha, \beta) \tag{4.16}$$

so the image of a point-source is a single point (perfect stigmatism): this is the case of geometric optics. Note that the same result is obtained if $\lambda \rightarrow 0$. The object-image relation becomes

$$I(\alpha, \beta) = I_0(-\alpha, -\beta) \tag{4.17}$$

so the image is the object itself (rotated by 180°).

4.2 Optical transfer function (OTF)

The convolution relationship in the focal plane (Eq. 4.15) corresponds to a linear filtering in the Fourier plane. If we denote u and v the *angular* frequencies associated with α and β , the Fourier transform of Eq. 4.15 becomes

$$\hat{I}(u, v) = \hat{I}_0(-u, -v) \cdot T(u, v) \tag{4.18}$$

with

$$T(u, v) = \mathcal{F}[S(\alpha, \beta)] = \mathcal{F}\left[\left|\hat{P}\left(\frac{\alpha}{\lambda}, \frac{\beta}{\lambda}\right)\right|^2\right] \tag{4.19}$$

The function $T(u, v)$ is called “Optical transfer function” (OTF). It is a complex function; its modulus and phase are denoted as “modulation transfer function” and “phase transfer function” respectively. u and v are expressed in rad^{-1} . To calculate $T(u, v)$, we use the Wiener-Kinchin theorem, which expresses the Fourier transform of the power spectrum of a function:

$$\mathcal{F}[|\hat{f}(u)|^2] = C_f(X) = \int_{-\infty}^{\infty} f(x) \overline{f(x+X)} dx \tag{4.20}$$

The quantity $C_f(X)$ is the *Autocorrelation function* of $f(x)$. It can be interpreted as the integral of superposition of the function $f(x)$ and the same function conjugated and translated: $\overline{f(x+X)}$.

Proof of the Wiener-Kinchin theorem:

- Write $|\hat{f}(u)|^2 = \hat{f}(u) \overline{\hat{f}(u)}$

¹To calculate the intensity created by the addition of several waves in incoherent light, one adds *intensities* of individual waves (not amplitudes).

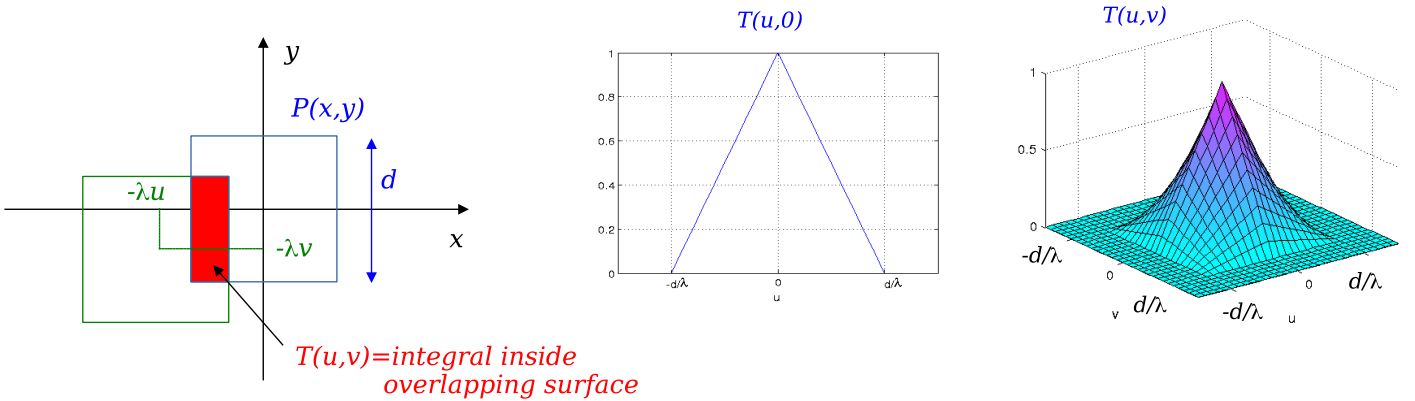


Figure 4.1: Illustration of the calculation of an Optical transfer function in the case of a square pupil of side d . Left: superposition of the overlapping terms: $P(x, y)$ (centered at $(0, 0)$) and $\bar{P}(x + \lambda u, y + \lambda v)$ (centered at $(-\lambda u, -\lambda v)$) which intervene in the integral of Eq. 4.26. Middle and right: plot of the OTF for $v = 0$ and in the (u, v) plane. The OTF is a pyramid in this case.

- Use the following Fourier properties :

$$\mathcal{F}[\hat{f}(u)] = f(-X) \quad (4.21)$$

and

$$\mathcal{F}[\overline{f(x)}] = \hat{f}(-u) \quad (4.22)$$

- The Fourier transform of $|\hat{f}(u)|^2$ is obtained as the convolution

$$C_f(X) = f(-X) * \overline{f(X)} \quad (4.23)$$

which develops as

$$C_f(X) = \int_{-\infty}^{\infty} f(-x') \overline{f(X-x')} dx' = \int_{-\infty}^{\infty} f(x) \overline{f(x+X)} dx \quad (4.24)$$

To compute the optical transfer function, we make use of the Wiener-Kinchin theorem and the Fourier property

$$\mathcal{F}\left[f\left(\frac{x}{a}\right)\right] = |a|\hat{f}(au)$$

so that

$$T(u, v) = \mathcal{F}\left[\left|\hat{P}\left(\frac{\alpha}{\lambda}, \frac{\beta}{\lambda}\right)\right|^2\right] = \lambda^2 C_P(\lambda u, \lambda v) \quad (4.25)$$

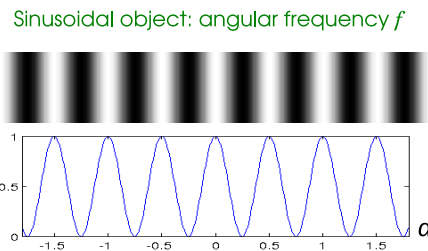
and in general we introduce a multiplicative constant to normalise the transfer function so that $T(0, 0) = 1$. We shall then define the OTF as

$$T(u, v) = \frac{1}{S} C_P(\lambda u, \lambda v) = \frac{1}{S} \iint_{-\infty}^{\infty} P(x, y) \overline{P(x + \lambda u, y + \lambda v)} dx dy \quad (4.26)$$

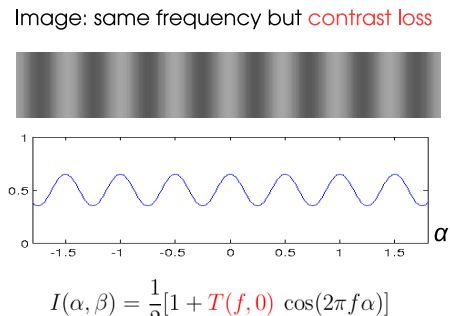
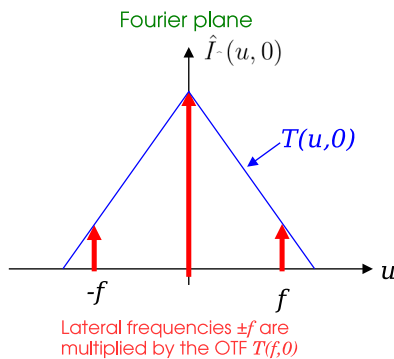
where S is the surface of the pupil. This is the integral of superposition of two identical pupils, one being conjugated and shifted by a quantity $(-\lambda u, -\lambda v)$ as illustrated by Fig. 4.1

Properties of the OTF:

- It is a normalised fonction $T(0, 0) = 1$
- If the pupil $P(x, y)$ is real, then the OTF $T(u, v)$ is **real and even**, $T(-u, -v) = T(u, v)$
- If the pupil is a separable function $P(x, y) = P_1(x).P_2(y)$ then the OTF is also a separable function $T(u, v) = \frac{1}{S} C_{P_1}(\lambda u).C_{P_2}(\lambda v)$
- If the pupil is isotropic (i.e. $P(x, y) = P(\rho)$ with $\rho^2 = x^2 + y^2$) then the OTF is also isotropic ($T(u, v) = T(q)$ with $q^2 = u^2 + v^2$)



$$I_0(\alpha, \beta) = \frac{1}{2} [1 + \cos(2\pi f\alpha)]$$



$$I(\alpha, \beta) = \frac{1}{2} [1 + T(f, 0) \cos(2\pi f\alpha)]$$

Figure 4.2: Illustration of the physical significance of the OTF in the case of an image of a sinusoidal grid. Left: object of intensity $I_0(\alpha, \beta)$. Middle: Fourier transform $\hat{I}(u, 0)$ together with the OTF $T(u, 0)$ (taken as a triangle for this example). Right: Observed image, with a contrast $|T(f, 0)|$.

Physical significance of the transfer function: To understand the physical significance of the OTF, let's consider an incoherent object which is a pure sinusoidal grid of angular frequency f in the α direction, as in Fig. 4.2. The object has an intensity distribution

$$I_0(\alpha, \beta) = \frac{1}{2} [1 + \cos(2\pi f\alpha)] \quad (4.27)$$

This object has indeed 3 vector angular frequencies in the (u, v) plane: $\vec{f}_1 = (0, 0)$, $\vec{f}_2 = (f, 0)$ and $\vec{f}_3 = (-f, 0)$. Its Fourier transform is

$$\hat{I}_0(u, v) = \frac{1}{2}\delta(u, v) + \frac{1}{4}\delta(u - f, v) + \frac{1}{4}\delta(u + f, v) \quad (4.28)$$

Applying the object-image relation in the Fourier plane (Eq. 4.18), we can derive the F.T. of the intensity distribution of the image:

$$\hat{I}(u, v) = \frac{T(0, 0)}{2}\delta(u, v) + \frac{T(f, 0)}{4}\delta(u - f, v) + \frac{T(-f, 0)}{4}\delta(u + f, v) \quad (4.29)$$

With $T(0, 0) = 1$ by definition. The lateral terms in $\hat{I}(u, v)$ are multiplied by *the value of the OTF at (u, v) equals to the grid frequencies*. In the case of an even OTF (corresponding to square or a circular pupil), we have $T(f, 0) = T(-f, 0)$ and the expression simplifies. It is then easy to obtain the image intensity distribution by inverse F.T.:

$$I(\alpha, \beta) = \frac{1}{2} [1 + T(f, 0) \cos(2\pi f\alpha)] \quad (4.30)$$

Which is also a sinusoidal grid of same frequency as the object. The difference is that the cosine term has been attenuated. The contrast of this figure is

$$C = \frac{I_{\max} - I_{\min}}{I_{\max} + I_{\min}} = |T(f, 0)| \quad (4.31)$$

which gives the physical significance of the OTF, in fact of its modulus (the MTF): it is indeed the contrast (also known as “visibility”) of the image of the grid. Changing the grid frequency would result into another value of the contrast. It is then possible to estimate the MTF by making images of grids of various frequencies and measure their contrast.

4.3 Case of a circular pupil

4.3.1 PSF and resolving power

The pupil is a uniform disc of diameter d . It expresses as

$$P(x, y) = \Pi\left(\frac{\rho}{d}\right) \quad \text{with } \rho^2 = x^2 + y^2 \quad (4.32)$$



the PSF is an Airy disc of intensity

$$S(\alpha, \beta) = \left(\frac{\pi d^2}{4}\right)^2 4 \operatorname{jinc}\left(\frac{\pi d \theta}{\lambda}\right)^2 \quad (4.33)$$

it is an isotropic function of the angle $\theta^2 = \alpha^2 + \beta^2$. It is independent of the telescope focal. The multiplicative constant $\left(\frac{\pi d^2}{4}\right)^2$ may be omitted. The PSF is displayed in Fig. 4.3. It exhibits a central peak of angular radius $1.22\frac{\lambda}{d}$ surrounded by dark and bright faint rings (the brightest ring has a maximum intensity of 1.7% of the peak intensity of the PSF).

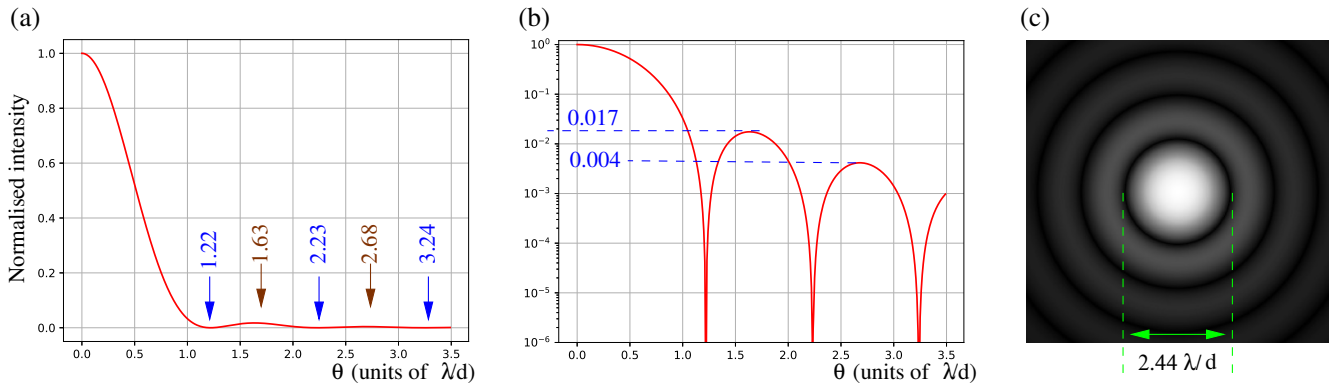


Figure 4.3: Airy disc: intensity PSF for a circular pupil of diameter d (Eq. 4.33). (a) plot of the intensity profile as a function of position angle θ in the focal plane. Positions of the first zeros and the first secondary maxima are written on the graph (in units of λ/d). (b) Same plot in semi-log scale. Relative intensities of the first secondary maxima are written on the graph. (c) Gray-level plot of the Airy disc.

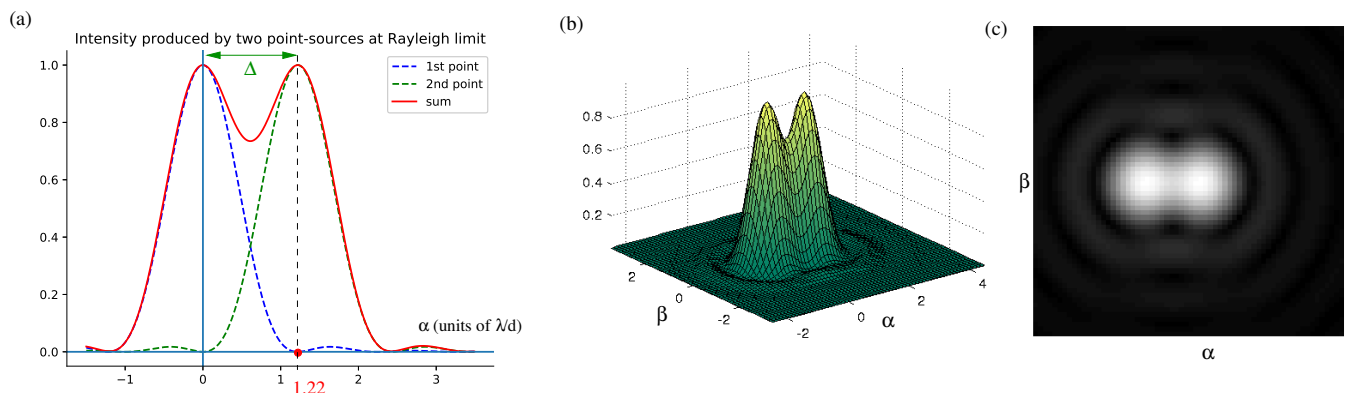


Figure 4.4: Image of two point-sources by a circular pupil at Rayleigh limit: star separation Δ is equal to the PSF radius $= 1.22\lambda/d$. (a) Plot of the intensity as a function of the angle α in the focal plane. (b) Surface plot of the intensity $I(\alpha, \beta)$. (c) Gray level plot of the intensity showing the aspect of the image.

Resolving power: it is defined from the image of two point-sources, composed by the sum of two shifted PSF. Images of each point-source are distinct if their separation is greater than the size of the PSF. An empiric definition was proposed by Lord Rayleigh in 1879 (*Phil. Mag. S 5. Vol. 8, Oct. 1879*). It corresponds to the situation where the angular separation Δ of the two points is exactly equal to the PSF radius, i.e. the radius of the first dark ring of the Airy disk (see Fig 4.4):

$$\Delta = 1.22 \frac{\lambda}{d} \quad [\text{unit: radian}] \quad (4.34)$$

Typical values for $\lambda = 500$ nm:

- $d = 12$ cm $\implies \Delta = 1$ arcsec
- $d = 2$ mm (human eye in daylight) $\implies \Delta = 1$ arcmin
- $d = 2.40$ m (Hubble Space Telescope) $\implies \Delta = 0.05$ arcsec

4.3.2 Optical transfer function

The OTF $T(u, v)$ is the surface of the intersection of two discs of diameter d , shifted by a vector $(\lambda u, \lambda v)$ as defined by Eq. 4.26. It is a real, isotropic function. The calculus is made in a geometrical way (see Goodman, “Introduction to Fourier Optics” for details) and gives a *chinese hat* function

$$T(u, v) = \text{rect}\left(\frac{\lambda q}{d}\right) \quad \text{with} \quad q^2 = u^2 + v^2 \quad (4.35)$$

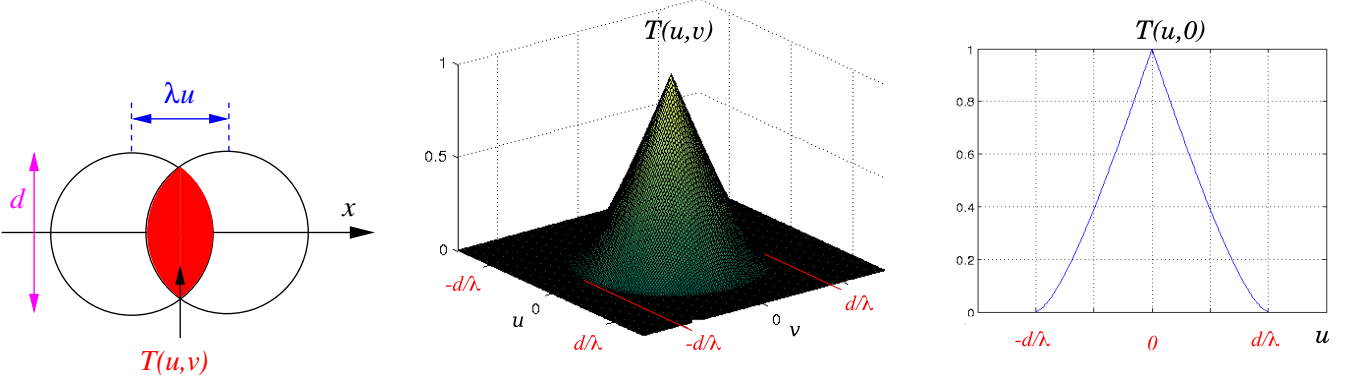
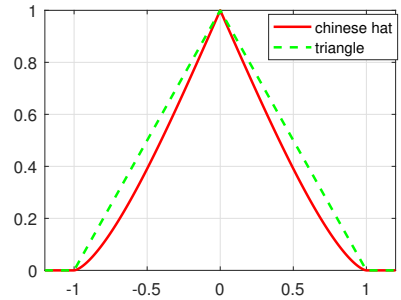


Figure 4.5: Transfer function of a circular pupil. Left: geometric interpretation of $T(u,v)$ as the area of the intersection of two identical shifted pupils (Eq. 4.26). Middle: 3D plot of the OTF showing the typical “chinese hat” shape. Right: Plot of $T(u,0)$, showing the angular cutoff frequency $f_c = d/\lambda$.

where

$$\text{大}(x) = \frac{2}{\pi} \left[\cos(|x|) - |x| \sqrt{1 - x^2} \right] \quad (4.36)$$

The function 大(x) is displayed on the right: it looks like a triangle with curved sides. It is an even function, vanishing for $|x| \geq 1$.



The graph of the transfer $T(u,v)$ function is shown in Fig. 4.5. It is an isotropic chinese hat which has non-zero values for $q \leq \frac{d}{\lambda}$. It corresponds to a low-pass filtering of angular frequencies of the object.

Cutoff frequency: it is defined as the highest frequency for which the transfer function is not zero. For a circular pupil of diameter d , the angular cutoff frequency is

$$f_c = \frac{d}{\lambda} \quad \text{unit: rad}^{-1} \quad (4.37)$$

The cutoff frequency is the frequency of the finest sinusoidal grid that the telescope is capable to image with non-zero contrast. In other words, if one considers a pure sinusoidal object having an intensity distribution $I_0(\alpha, \beta) = A \cos(\pi u_0 \alpha)^2$ of angular frequency u_0 , then its image becomes uniform when $u_0 \geq d/\lambda$.

It is possible to use f_c to define a resolving power in a sense less empirical than the Rayleigh criterion presented before. Let's define $\Delta_c = \frac{1}{f_c}$ the *cutoff period*, i.e. the angular period of the finest imageable grid. Indeed, Δ_c represents the angular size of the finest details in the image: this gives another definition of the resolving power for a pupil of diameter d :

$$\Delta_c = \frac{\lambda}{d} \quad (4.38)$$

It is sometimes called “resolution element” or *resel*. We see that Δ_c is close to the Rayleigh definition $\Delta = 1.22 \frac{\lambda}{d}$. Note that

- When $d \nearrow$ then $\Delta_c \searrow$: better resolution for a large telescope
- When $\lambda \searrow$ then $\Delta_c \searrow$: better resolution at short wavelengths